Copy 1
RM E54J11

NACA RM E54J11

NACA

RESEARCH MEMORANDUM

EXPERIMENTAL DETERMINATION OF LINEAR DYNAMICS OF TWO-SPOOL TURBOJET ENGINES

By David Novik and Herbert Heppler

Lewis Flight Propulsion Laboratory
Cleveland, Ohio

NATIONAL ADVISORY COMMITTEE FOR AERONAUTICS

WASHINGTON

ERRATA

NACA RM E54J11

EXPERIMENTAL DETERMINATION OF LINEAR DYNAMICS OF

TWO-SPOOL TURBOJET ENGINES

By David Novik and Herbert Heppler

Equations (A7) to (A15) should be changed to the following forms. (These changes consist essentially of differences in sign in the numerators.)

Page 18:

$$\left|\frac{\Delta N_o}{\Delta T_4}\right|_A = -\frac{q_{T_4}}{q_{N_o}} \frac{\left(\frac{-I_i}{Q_{N_i}} p + 1\right) - \frac{Q_{T_4} q_{N_i}}{Q_{N_i} q_{T_4}}}{\left(\frac{-I_i}{Q_{N_i}} p + 1\right)\left(\frac{-I_o}{q_{N_o}} p + 1\right) - \frac{Q_{N_o} q_{N_i}}{Q_{N_i} q_{N_o}}} \tag{A7}$$

Page 19:

$$\left|\frac{\Delta N_i}{\Delta T_4}\right|_A = -\frac{Q_{T_4}}{Q_{N_i}} \frac{\left(\frac{-I_o}{q_{N_o}} p + 1\right) - \frac{Q_{N_o} q_{T_4}}{q_{N_o} Q_{T_4}}}{\left(\frac{-I_i}{Q_{N_i}} p + 1\right)\left(\frac{-I_o}{q_{N_o}} p + 1\right) - \frac{Q_{N_o} q_{N_i}}{Q_{N_i} q_{N_o}}} \tag{A8}$$

Page 19:

$$\left|\frac{\Delta N_o}{\Delta T_4}\right|_A = -\frac{q_{T_4}}{q_{N_o}} \frac{(\tau_i p + 1) - \frac{Q_{T_4} q_{N_i}}{Q_{N_i} q_{T_4}}}{(\tau_i p + 1)(\tau_o p + 1) - \frac{Q_{N_o} q_{N_i}}{Q_{N_i} q_{N_o}}} \tag{A9}$$

Page 19:

$$\left|\frac{\Delta N_i}{\Delta T_4}\right|_A = -\frac{Q_{T_4}}{Q_{N_i}} \frac{(\tau_o p + 1) - \frac{Q_{N_o} q_{T_4}}{q_{N_o} Q_{T_4}}}{(\tau_i p + 1)(\tau_o p + 1) - \frac{Q_{N_o} q_{N_i}}{Q_{N_i} q_{N_o}}} \tag{A10}$$

Page 19:

$$\left|\frac{\Delta N_o}{\Delta A}\right|_{T_4} = -\frac{q_A}{q_{N_o}} \frac{(\tau_i p + 1) - \frac{Q_A q_{N_i}}{Q_{N_i} q_A}}{(\tau_i p + 1)(\tau_o p + 1) - \frac{Q_{N_o} q_{N_i}}{Q_{N_i} q_{N_o}}} \qquad \text{(A11)}$$

Page 19:

$$\left|\frac{\Delta N_i}{\Delta A}\right|_{T_4} = \frac{-\frac{Q_A}{Q_{N_i}}(\tau_o p + 1) + \frac{Q_{N_o} q_A}{Q_{N_i} q_{N_o}}}{(\tau_i p + 1)(\tau_o p + 1) - \frac{Q_{N_o} q_{N_i}}{Q_{N_i} q_{N_o}}} \qquad \text{(A12)}$$

Pages 7, 9, 20:

$$\left|\frac{\Delta N_o}{\Delta T_4}\right|_A = -\frac{q_{T_4}}{q_{N_o}} \frac{(\tau_i p + 1) - \frac{Q_{T_4} q_{N_i}}{Q_{N_i} q_{T_4}}}{(\tau_i p + 1)(\tau_o p + 1)} \qquad \text{(A13)}$$

Pages 7 and 20:

$$\left|\frac{\Delta N_i}{\Delta T_4}\right|_A = -\frac{Q_{T_4}}{Q_{N_i}} \frac{1}{\tau_i p + 1} \qquad \text{(A14)}$$

Pages 7 and 20:

$$\left|\frac{\Delta N_o}{\Delta A}\right|_{T_4} = -\frac{q_A}{q_{N_o}} \frac{1}{\tau_o p + 1} \qquad \text{(A15)}$$

Page 9: The two equations following equation (A13) should be:

$$(\tau_i p + 1) + \frac{Q_{T_4} q_{N_i}}{Q_{N_i} q_{T_4}} \cong \tau_o p + 1$$

and

$$\left|\frac{\Delta N_o}{\Delta T_4}\right|_A \cong -\frac{q_{T_4}}{q_{N_o}} \frac{1}{\tau_i p + 1}$$

Pages 10 and 12: In all the equations on these pages, the proportionality signs $\propto$ should be changed to equality signs $=$.

NATIONAL ADVISORY COMMITTEE FOR AERONAUTICS

RESEARCH MEMORANDUM

EXPERIMENTAL DETERMINATION OF LINEAR DYNAMICS OF TWO-SPOOL TURBOJET ENGINES

By David Novik and Herbert Heppler

SUMMARY

An experimental determination of the dynamics of two-spool turbojet engines is presented. Step inputs in fuel flow and in exhaust-nozzle area were utilized for initiation of transients on a test engine; and the resultant transient data were analyzed with fuel flow, turbine-inlet temperature, and exhaust-nozzle area considered as independent variables. Transfer functions, descriptive of general response, were obtained for the more important engine variables.

From the test-program data, the speed responses of both spools to changes in turbine-inlet temperature appeared to be first-order lag systems with the same time constants. Data presented for another two-spool turbojet engine of different manufacture indicated that the speed responses of the two spools to changes in fuel flow also were identical first-order lags.

With respect to exhaust-nozzle area changes, it was found that the outer-spool response appeared to be a first-order lag. Response of the inner spool near rated speed was apparently second order, but the magnitude of change in the operating region was so small as to have no appreciable effect on the first-order outer-spool response or on the response of other engine variables.

Comparison of engine response to the independent variables, turbine-inlet temperature (or fuel flow) and exhaust-nozzle area, indicated that engine dynamics for changes in turbine-inlet temperature (or fuel flow) were functions of inner-spool response and that engine dynamics for changes in exhaust-nozzle area were functions of outer-spool response. The engine responded more rapidly to a change in exhaust-nozzle area than to a change in turbine-inlet temperature or fuel flow. Experimental speed responses were found to agree with analytically derived equations of response.

INTRODUCTION

In general, determination of the dynamics of an engine, supplemented by knowledge of the steady-state engine performance, is considered to be a prerequisite to the successful design of an optimum engine control system. Linear dynamics are considered necessary for stability and control-parameter considerations, and nonlinear dynamics are vital for delineation of surge limits and maximum acceleration potential.

Sufficient effort has already been expended on the determination of single-spool turbojet- and turboprop-engine dynamics so that these engines are generally accepted as first-order lag systems whose responses can be characterized by means of time constants. The addition of the two-spool engine to those powerplants currently available for military aircraft use introduces an engine that contains an energy storage element with each spool and hence is inherently at least a second-order system. Published information pertinent to the dynamics of the two-spool engine has thus far been relatively scarce.

At the NACA Lewis laboratory, experimental programs have been undertaken for the purpose of obtaining both linear and nonlinear dynamics of two-spool engines, in conjunction with steady-state performance under varying conditions of operation. The scope of this report is confined to an investigation of the linear dynamics of two-spool engines with the expectation that the information presented will be useful in control synthesis from stability and control-parameter considerations. A two-spool engine, operated in a sea-level test stand, was subjected to step inputs in fuel flow and exhaust-nozzle area. Some of the original transient data obtained are presented, together with typical results of harmonic analysis of the data and the transfer functions of the engine variables derived therefrom. An acceleration trace for a two-spool engine of different manufacture is also shown and analyzed.

SYMBOLS

The following symbols are used in this report:

A	exhaust-nozzle area
a	rise ratio
F	thrust
I	moment of inertia
K	constant

N	engine speed
P	total pressure
p	differential operator
T	total temperature
t	time
W_f	fuel flow
y_f	engine variable at end of transient
y_t	engine variable at time equals t
y_0	engine variable at time equals zero
δ	pressure correction, ratio of ambient pressure to NACA standard sea-level pressure
θ	temperature correction, ratio of ambient temperature to NACA standard sea-level temperature
τ	time constant with T_4 and A considered as independent variables
τ'	time constant with W_f and A considered as independent variables
φ	phase shift, deg
ω	frequency, radians/sec

Subscripts:

i	inner
o	outer
1	outer-compressor inlet
2	outer-compressor discharge and inner-compressor inlet
3	inner-compressor discharge
4	turbine inlet
9	tail pipe

Functions, transfer functions, and partial derivatives:

Q inner-spool torque expressed as function of N_o, N_i, T_4, and A

Q' inner-spool torque expressed as function of N_o, N_i, W_f, and A

q outer-spool torque expressed as function of N_o, N_i, T_4, and A

q' outer-spool torque expressed as function of N_o, N_i, W_f, and A

$\left|\frac{\Delta q}{\Delta T_4}\right|_A$ transfer function for response of outer-spool torque to a change in turbine-inlet temperature at constant exhaust-nozzle area

$$q_{N_o} = \left(\frac{\partial q}{\partial N_o}\right)_{N_i,T_4,A}$$

$$q'_{N_o} = \left(\frac{\partial q'}{\partial N_o}\right)_{N_i,W_f,A}$$

APPARATUS

Engine

The two-spool engine used in this investigation is presented schematically in figure 1. The engine is essentially composed of an outer axial-flow compressor connected by a through shaft to a turbine, an inner compressor connected to a turbine, and a multiunit semiannular combustion chamber. Automatic bleed valves, closed during high-speed operation and open at low speeds, are located between the two compressors. Experimentally determined steady-state performance curves are shown in figure 2 as functions of inner-spool speed.

Fuel System

The engine fuel system, up to the flow divider, was supplanted by a test-facility fuel system as shown in figure 3. The fuel control consisted of a differential relief valve controlling the pressure drop across a throttle valve, the position of which (and thus the area) was varied by an electrohydraulic servomotor. In such a system, fuel flow is proportional to throttle-valve position. The natural frequency of the differential relief valve was approximately 250 cycles per second (ref. 1), and the natural frequency of the electrohydraulic servomotor was approximately 60 cycles per second. Because of the high natural

frequency of the differential relief valve, the fuel flow was proportional to the throttle-valve position for all throttle-valve transients. Therefore, throttle-valve position was used as the recorded indication of fuel flow. The over-all response of the fuel system, up to the engine flow divider, was underdamped but reached equilibrium within 0.03 second following a step input.

Variable Exhaust-Nozzle Area

Exhaust-nozzle area was varied by means of pneumatically operated flaps as shown in figure 4. The two flaps were linked together so that they moved simultaneously, and motion of the flaps from open to closed approximated a ramp of about 0.04 to 0.05 second.

Engine speeds. - Transients in engine speeds were measured by recording the d-c voltage outputs of electronic counters that counted the pulses supplied from 180-tooth tachometer generators. Before recording, the speed signals were filtered with resistance-inductance-capacitance filters that had characteristics as shown in figure 5.

Engine temperatures. - Temperatures at the discharge of the outer and inner compressors were measured by three iron-constantan thermocouples in series at each station. Thermocouples were made of 27-gage wire and ground to a sharp arrowhead point for fast response without compensation.

Turbine-inlet and tail-pipe temperatures were measured by three chromel-alumel thermocouples in series at each station. These high-temperature thermocouples were made of 14-gage wire and were compensated. The compensated signal to the recorder had a lag of approximately 0.03 second.

Engine pressures. - Engine pressures were measured by means of strain-gage pressure pickups. Pressure responses had apparent time constants below 0.01 second.

Thrust. - Engine thrust was measured by a strain-gage thrust link.

EXPERIMENTAL PROCEDURE AND DATA

Test Procedure

Data indicative of the response of outer-spool speed, inner-spool speed, outer-compressor-discharge pressure and temperature, inner-compressor-discharge pressure and temperature, turbine-inlet temperature, tail-pipe pressure, tail-pipe temperature, and thrust were recorded during transients induced by changes in fuel flow and exhaust-nozzle area.

Fuel-flow transients. - Fuel-flow transients, covering a range of engine speeds, were initiated from approximate step inputs in fuel flow. Fuel changes were of such a magnitude as to result in inner-spool speed changes of approximately 3 percent on the assumption that these speed changes were small enough to insure linearity. Exhaust-nozzle area was fixed during fuel-flow transients.

Exhaust-nozzle-area transients. - Exhaust-nozzle-area transients were induced by closing the flaps installed on the exhaust nozzle. Closing the flaps corresponded to a change in exhaust-nozzle area from 105 percent area to 100 percent area and resulted in outer-spool speed changes of about 3 percent. Fuel flow was maintained constant during exhaust-nozzle-area transients.

3485

Transient Data

Fuel-flow transient data. - Samples of transient data obtained for approximate step inputs in fuel flow are shown in figures 6(a) and (b). It is of interest to note that both spools appear to move simultaneously as though the rotors were geared together. An increase in response time is evident for the transient at the lower engine speed.

Figure 6(c) has been included to illustrate the discontinuities in the engine variables when the compressor bleed valves automatically close during a transient.

Exhaust-nozzle-area transient data. - Typical transient data obtained for approximate steps (ramps of 0.04 to 0.05 sec) in exhaust-nozzle area are shown in figure 7. In all the transients shown, the exhaust nozzle went from an open to a closed position. Area traces may be erratic or are not recorded at all because of a faulty potentiometer coupling.

Inspection of exhaust-nozzle-area transients reveals that the inner-spool response is of extremely small magnitude except at the low engine speeds and that its net change near top speeds is opposite in direction from that of the outer spool. Net changes in thrust for changes in exhaust-nozzle area are always small, despite the initial response.

ANALYSIS OF DATA

Theoretical Analysis

In order to facilitate evaluation of the experimental data obtained, reference is made to the following equations of response. These equations

are derived in appendix A for engine operation near rated speed.

$$\left|\frac{\Delta N_o}{\Delta T_4}\right|_A = \frac{q_{T_4}}{q_{N_o}} \frac{(\tau_i p + 1) + \frac{Q_{T_4} q_{N_i}}{Q_{N_i} q_{T_4}}}{(\tau_i p + 1)(\tau_o p + 1)} \tag{A13}$$

$$\left|\frac{\Delta N_i}{\Delta T_4}\right|_A = \frac{Q_{T_4}}{Q_{N_i}} \frac{1}{\tau_i p + 1} \tag{A14}$$

$$\left|\frac{\Delta N_o}{\Delta A}\right|_{T_4} = \frac{q_A}{q_{N_o}} \frac{1}{\tau_o p + 1} \tag{A15}$$

$$\left|\frac{\Delta N_i}{\Delta A}\right|_{T_4} = \frac{\frac{Q_{N_o} q_A}{Q_{N_i} Q_{N_o}}}{(\tau_i p + 1)(\tau_o p + 1)} \cong 0 \tag{A16}$$

where $\tau_o = -\frac{I_o}{q_{N_o}}$ and $\tau_i = -\frac{I_i}{Q_{N_i}}$.

Although equations (A13) to (A16) specify turbine-inlet temperature rather than fuel flow as an independent variable, these equations are also indicative of fuel-flow response near rated speed because turbine-inlet temperature response to fuel flow normally approaches unity near rated engine speed.

Response of Engine Variables to Fuel Flow from Harmonic Analysis of Transient Data

Typical frequency-response curves obtained from harmonic or Fourier analysis (ref. 2) of fuel step transients are shown in figures 8 and 9. Frequencies corresponding to the points shown are given in table I. Cursory examination of these frequency-response curves shows higher-order responses that are obviously not in agreement with the responses anticipated from analysis. For example, it can be seen that the inner-spool speed response, even at high speed, appears to be considerably more complex than the anticipated approximation of first-order response.

It is believed that the apparent discrepancy between analysis and data can be attributed to incomplete combustion during initial phases of the transients, and possibly to dynamics of the spring-loaded flow divider. Combustion dynamics are implied from inspection of figure 8(g), which shows the response of turbine-inlet temperature to fuel flow at 96.1 percent rated inner-spool speed. The large phase shifts evident at high frequencies cannot be attributed to engine-speed dynamics because the speed responses are very much attenuated at the high frequencies. The higher-order phase shifts in the temperature response must therefore be indicative of combustion lags immediately following the fuel step.

Despite the combustion effects, some general trends in the responses to fuel flow can be ascertained. The frequency-response curves of the two speeds (figs. 8(a) and (b) or 9(a) and (b)) are essentially the same, indicating that one transfer function defines the response of both spools. Smaller phase shifts for other engine variables are indicative of leads in the response of these variables as compared with the speed response. Engine response is slower at the lower engine speeds as evidenced by the increased phase shift for a given frequency at the lower engine speed.

The transient data of figure 10, taken from a two-spool turbojet engine of different manufacture than the test engine, can be analyzed to give more valid indications of response to fuel flow because of the slower rate of fuel addition. The frequency-response curves of outer- and inner-spool speeds with respect to fuel flow for these data are shown in figure 11. It can be seen that the responses of both spools appear to be identical first-order lags. The response of the inner spool is therefore in agreement with the response anticipated from equation (A14). The response of the outer spool, however, is simpler than anticipated by equation (A13) in that it is the same first-order lag as that of the inner spool.

Response of Engine Variables to Turbine-Inlet Temperature from Harmonic Analysis of Transient Data

Inasmuch as the turbine-inlet temperature reflects the amount of energy actually available for acceleration, the frequency response of engine variables with respect to turbine-inlet temperature can be expected to yield more predictable results than the responses to fuel-flow changes.

Typical frequency-response curves showing the responses of engine variables to turbine-inlet temperature (obtained from harmonic analysis of the fuel-step transient data with reference to turbine-inlet temperature as the input) are shown in figures 12 and 13.

Speed responses. - The frequency responses of outer-spool speed to turbine-inlet temperature are shown in figures 12(a) and 13(a), and the responses of inner-spool speed are shown in figures 12(b) and 13(b). The responses of both spools appear to be first order, and the indicated time constants $\left(\tau = \frac{1}{\text{frequency at } 45^\circ \text{ phase shift}}\right)$ of each spool are almost identical. The response of both spools to turbine-inlet temperature appears to be

$$\frac{\Delta N}{\Delta T_4} = \frac{K}{\tau p + 1}$$

where K represents the steady-state gain of the spool being considered and τ represents a time constant common to both spools.

The experimental response of inner-spool speed to changes in turbine-inlet temperature therefore agrees with the analysis (eq. (A14)) in that it is a first-order response with a time constant $\tau_i = \frac{-I_i}{Q_{N_i}}$. The fact that the experimental response of outer-spool speed appears to be virtually the same as the response of inner-spool speed means that the second-order system of equation (A13) must degenerate into a first-order system with a time constant τ_i. It is assumed that this simplification occurs in the following manner:

$$\left|\frac{\Delta N_o}{\Delta T_4}\right|_A = \frac{q_{T_4}}{q_{N_o}} \frac{(\tau_i p + 1) + \frac{Q_{T_4} q_{N_i}}{Q_{N_i} q_{T_4}}}{(\tau_i p + 1)(\tau_o p + 1)} \qquad \text{(A13)}$$

but apparently

$$(\tau_i p + 1) + \frac{Q_{T_4} q_{N_i}}{Q_{N_i} q_{T_4}} \propto \tau_o p + 1$$

and therefore

$$\left|\frac{\Delta N_o}{\Delta T_4}\right|_A \propto \frac{q_{T_4}}{q_{N_o}} \frac{1}{\tau_i p + 1}$$

Inasmuch as figure 11 has already indicated similar responses for the two spools of an entirely different engine, the preceding factoring may be considered more of a generality than a coincidence.

A plot of the variation of the inner-spool time constant τ_i as a function of inner-spool speed N_i (measured at the end of each transient) is shown in figure 14. Variation of the apparent time constants τ obtained for the outer-spool response to turbine-inlet temperature is also shown. Figure 14 shows no appreciable difference between the two responses although there appears to be a very slight tendency for the inner spool to be slower than the outer spool at high speeds. Compressor bleed at 92.5 percent rated inner-spool speed is seen to reduce the time constant by an almost negligible amount. The over-all trend of both spools exhibits the usual variation of response time with engine speed normally associated with single-spool turbojet engines.

Outer-compressor-discharge pressure response. - Response of outer-compressor-discharge pressure P_2 to changes in turbine-inlet temperature at constant area (figs. 12(c) and 13(c)) appears to have a small lead with respect to the speed response. In transfer function form,

$$\left|\frac{\Delta P_2}{\Delta T_4}\right|_A \propto \frac{K(a\tau_i p + 1)}{\tau_i p + 1} \propto \frac{K\left(\tau_{P_2} p + 1\right)}{\tau_i p + 1}$$

The value of a (or $\frac{\tau_{P_2}}{\tau_i}$) is the rise ratio obtained from the frequency-response curve such that $a = \frac{\tau_{P_2}}{\tau_i} = \frac{\text{amplitude at infinite frequency}}{\text{amplitude at zero frequency}}$. (Where higher-order lags appear, they are neglected and the amplitude at infinite frequency is taken at the point of intersection of the faired curve with the zero phase-shift axis.) Variation of rise ratio with engine speed is shown in figure 15, from which it may be seen that the rise ratios are small and disappear at low engine speeds.

Outer-compressor-discharge temperature response. - The outer-compressor-discharge temperature T_2 exhibits a small degree of lead as shown in figures 12(d) and 13(d). Data were too inconclusive to permit a plot of rise ratios; however, a rise ratio of approximately 0.1 is estimated at rated speed. It is assumed that the trend of rise ratios with engine speed is similar to that shown for outer-compressor-discharge pressure (fig. 15).

Inner-compressor-discharge pressure response. - Figures 12(e) and 13(e) indicate that the response of inner-compressor-discharge pressure P_3 to turbine-inlet temperature at constant area is a lead-lag system that can be approximated by the relation

$$\left|\frac{\Delta P_3}{\Delta T_4}\right|_A \propto \frac{K(a\tau_i p + 1)}{\tau_i p + 1} \propto \frac{K\left(\tau_{P_3} p + 1\right)}{\tau_i p + 1}$$

Values of rise ratio for inner-compressor-discharge pressure as a function of engine speed are shown in figure 16, from which it can be seen that the rise ratio is small and increases with increasing engine speed.

Inner-compressor-discharge temperature response. - The response of inner-compressor-discharge temperature to turbine-inlet temperature appears to be a lead-lag system (figs. 12(f) and 13(f)) as would be expected from the lead-lag response obtained for inner-compressor-discharge pressure. The temperature rise ratios are plotted in figure 17 and apparently are quite small with a very slight increase at increasing engine speed.

Tail-pipe pressure response. - Figures 12(g) and 13(g) show that the tail-pipe pressure response to a change in turbine-inlet temperature appears to be a lead-lag system with small rise ratios. As shown in figure 18, the rise ratio increases with increasing engine speed.

Tail-pipe temperature response. - Rise ratios indicative of tail-pipe temperature lead-lag response can be obtained from figures 12(h) and 13(h). If the premise is accepted that combustion within the combustors was incomplete, then roughness of the data in the frequency-response curves is a reasonable result. Large rise ratios that decreased with increasing engine speed were obtained as shown in figure 19.

Thrust response. - Thrust response to turbine-inlet temperature (figs. 12(i) and 13(i)) appears to be lead-lag. Variation of rise ratio with engine speed is shown in figure 20. Rise ratios are small and increase with increasing engine speed.

Effect of large fuel steps on appearance of lead response. - In order to approach linearity, small steps in fuel flow were used to initiate the transients. The over-all changes in engine variables were therefore small, and the leads or immediate changes inherent in the dynamics of some engine variables are not visibly apparent in the transient data. The leads become more obvious for large fuel steps, as shown in figure 21, in which the leads in turbine-inlet temperature, tail-pipe temperature, thrust, and inner-compressor-discharge pressure can be clearly seen.

Response of Engine Variables to Changes in Exhaust-Nozzle Area from Harmonic Analysis of Transient Data and from Semilog Plots

Illustrative frequency-response curves showing the response of engine variables to steps in exhaust-nozzle area at constant fuel flow are shown in figures 22 to 25. These curves were obtained from harmonic analysis of the transient data shown in figure 7. Inspection of these frequency-response curves indicates characteristic responses that appear to be very

close to first order. Inasmuch as first-order exponential curves plot as straight lines on semilog paper, the transients of figure 7 have been normalized according to figure 26 and plotted on semilog paper in figures 27 to 30. Scatter of data toward the end of the semilog plots is considered to be the result of engine drift and difficulty of measurement, in addition to small higher-order engine dynamics.

Outer-spool speed response. - Response of outer-spool speed to changes in exhaust-nozzle area at constant fuel flow is characterized by a 90° phase-shift semicircle in the frequency-response plots (figs. 22(a), 23(a), 24(a), and 25(a)) and by a straight line on the semilog plots (figs. 27 to 30). Both methods of data analysis are therefore indicative of first-order response and tend to corroborate the response anticipated from equation (A15). This response is now at constant fuel flow rather than constant turbine-inlet temperature:

$$\left|\frac{\Delta N_o}{\Delta A}\right|_{W_f} \propto \frac{K}{\tau_o' p + 1}$$

where $\tau_o' = \frac{-I_o}{q'_{N_o}}$

A plot of time constants for the response of outer-spool speed to exhaust-nozzle area, as obtained from frequency-response curves and from semilog plots, is shown in figure 31, as a function of engine speed. The time constants decrease as engine speed increases, and the response is essentially constant in the top-speed range.

Inner-spool speed response. - Inner-spool speed response to changes in exhaust-nozzle area is considerably different from the response of outer-spool speed. As noted previously in the discussion of the transient data, the steady-state gain or net change of the inner spool is in the same direction as that of the outer spool at low speeds (speeds below normal operating range), is rather indecisive and small at about 85 to 90 percent of rated outer-spool speed (fig. 7(b)), and is small and opposite in direction at speeds approaching rated speed (fig. 7(a)).

The semilog plot (fig. 27) and the frequency-response curve (fig. 22(b)) for the transient most closely approaching rated speed indicate that the inner-spool speed response is second order near rated speed. It is surmised that the transfer function of inner-spool speed is (from eq. (A16))

$$\left|\frac{\Delta N_i}{\Delta A}\right|_{W_f} \propto \frac{K}{(\tau_i' p + 1)(\tau_o' p + 1)}$$

Although the inner spool has a dynamic response to changes in exhaust-nozzle area, as approximated in the preceding equation, the steady-state gain or net change is so small as to leave the outer-spool speed essentially unaffected and, to all outward appearances, first order.

From near rated speed to the vicinity of 65 percent rated speed (based on outer-spool speed), there is a gap in which the change in inner-spool speed with exhaust-nozzle area is small and inner-spool dynamics are essentially negligible and indeterminate. This region is typified by the transient of figure 7(b) and by the responses shown in figures 23 and 28. The essentially first-order appearance of outer-spool speed indicates that the change in inner-spool speed is too small to have any measurable effect.

In the vicinity of 65 percent rated outer-spool speed, the inner-spool response to exhaust-nozzle area appears first order with a longer time constant than that of the outer spool (figs. 24(b) and 29). The response is large enough to have a small effect on the outer-spool speed, toward the end of the transient, as indicated by the break in slope of the outer-spool speed in figure 29.

At the lowest speed for which transient data were obtained (fig. 7(d)), corresponding to a final outer-spool speed of 44.7 percent of rated, the inner-spool response continued to appear first order (figs. 25(b) and 30). The magnitude of change has increased to approximately the same as that of the outer spool, and the time constant has become identical to that of the outer spool.

Basic engine response to change in exhaust-nozzle area. - Plots of engine variables (other than speed) in figures 27 to 30 fall parallel to the outer-spool speed traces, and in figures 22 to 24 the maximum amplitudes of the engine variables occur at frequencies that correspond to the outer-spool time constants. The inner-spool dynamics therefore have essentially no effect on the dynamics of the engine variables, and rise ratios can be obtained on the premise that the first-order lag of the outer spool represents the basic engine response.

Outer-compressor-discharge pressure response. - The frequency-response curves of figures 22(c), 23(b), and 24(c) show no definite dynamics in outer-compressor-discharge pressure response other than the first-order speed lag. The semilog plots of figures 27 to 30 show indications of a slight lead with respect to speed, but it is believed that this is because compensation was not made for the lags in the speed traces. It is concluded that the response of outer-compressor-discharge pressure to changes in exhaust-nozzle area is basically a first-order lag that follows the change in outer-spool speed.

Outer-compressor-discharge temperature response. - Response of outer-compressor-discharge temperature to changes in exhaust-nozzle area may be seen from the frequency-response plots of figures 22(d) and 23(c) and from the semilog curves of figures 27 and 28. As in the response of the outer-compressor pressure, the temperature appeared to follow the outer-spool speed without additional dynamics. Transient data for outer-compressor-discharge temperature were subject to large fluctuations such that analysis in some cases was impossible, and the faired curves used in analysis of the data must be construed as rough approximations.

Inner-compressor-discharge pressure response. - Response of inner-compressor-discharge pressure to changes in exhaust-nozzle area may be seen from the frequency-response curves of figures 22(e), 23(d), and 24(d) and from the semilog plots of figures 27 to 30. The response apparently follows that of the outer spool without any other dynamics, despite inner-spool speed dynamics.

Inner-compressor-discharge temperature response. - The original transient-data traces of inner-compressor-discharge temperature were subject to large fluctuations such that some traces could not be faired at all for analysis and other faired traces were rough approximations. Typical analyzed responses obtained are shown in the frequency-response curves of figures 22(f) and in the semilog plot of figure 27. The response of inner-compressor-discharge temperature appears to be the same as that of the outer-spool speed.

Turbine-inlet temperature response. - The frequency-response curves of turbine-inlet temperature (figs. 22(g), 23(e), and 24(e)) and the semilog plots of figures 27 to 29 indicate that turbine-inlet temperature response to exhaust-nozzle area is a lead-lag system.

The rise ratios (indicative of initial jump) are very small and approach zero in the top-speed range. The small values of rise ratio coupled with the fact that the steady-state change with area is small implies that for small changes in exhaust-nozzle area the turbine-inlet temperature response could probably be assumed to be zero. Rise ratios obtained are plotted in figure 32.

Tail-pipe pressure response. - Response of tail-pipe pressure to exhaust-nozzle area may be seen from the frequency-response curves of figures 22(h), 23(f), and 24(f) and from the semilog plots of figures 27 to 30. Tail-pipe pressure response has a very definite lead as expected for exhaust-nozzle area changes. The second-order lags noticeable at the high-frequency end of some of the frequency-response curves may possibly be attributed to inner-spool speed changes. If these second-order effects are neglected, a plot of rise ratios for tail-pipe pressure as a function of engine speed is obtained as shown in figure 33. No discernible trend in rise ratio was found.

Tail-pipe temperature response. - Tail-pipe temperature response to changes in exhaust-nozzle area is indicated by the frequency-response curves of figures 22(i), 23(g), and 24(g) and by the semilog plots of figures 27 to 29. A small amount of lead is apparent in the response and the lag decay follows outer-spool speed.

A first-order lead-lag system is used as an approximation of the response, and rise ratios are small and increase with increasing engine speed. The estimated point shown in figure 34 is the result of allowance made for the fact that electrical compensation was not used to correct for thermocouple lag in the tail-pipe temperature measurement of the transient shown in figure 7(a). Inasmuch as the thermocouple time constant could be reasonably estimated at 0.3 second and yet the phase shift resulting from this 0.3-second lag was more than cancelled out by the lead of the calculated response (fig. 22(i)), it was assumed that the lead time constant must have been at least 0.3 second.

Thrust response. - Frequency-response curves for the response of thrust to changes in exhaust-nozzle area are shown in figures 22(j), 23(h), and 24(h), and relative slopes are shown in the semilog plots of figures 27 to 29. If positive rise ratios are assumed for the condition in which the final value of thrust exceeds the initial value of thrust for a reduction in exhaust-nozzle area, then the rise ratios were found to be positive at the low engine speeds and negative at the high engine speeds. A plot of rise ratio as a function of engine speed is shown in figure 35. Infinite values of rise ratio indicate a condition in which initial and final values of thrust are identical. The initial jumps in thrust, corresponding to 5-percent exhaust-nozzle area changes, were on the order of 5 percent.

Transfer Functions

Responses of all engine variables investigated have been approximated as transfer functions and are listed in table II. The transfer functions are based on the inner-spool time constant for fuel flow and turbine-inlet temperature inputs and are based on the outer-spool time constant for exhaust-nozzle area inputs.

Relative Response

Comparison of the time-constant curves of figures 14 and 32 shows that the engine responds more rapidly to a change in exhaust-nozzle area than it does to a change in turbine-inlet temperature. Near rated speed, the response of turbine-inlet temperature to fuel flow approaches unity (fig. 8(g)) and, hence, engine response to exhaust-nozzle area is also faster than the response to fuel flow, at least near rated speed.

It may also be concluded that if each spool is taken as a separate entity, the outer spool has a smaller time constant (or energy storage element) than the inner spool. This is deduced from the fact that engine response to changes in exhaust-nozzle area is a function of outer-spool time constant, whereas engine response to changes in fuel flow appears to be a function of inner-spool time constant.

SUMMARY OF RESULTS

Transient data obtained from step inputs in fuel flow and exhaust-nozzle area for sea-level operation of a two-spool turbojet engine have been presented and analyzed. Because the fuel steps resulted in a non-linear time variable relation between fuel flow and turbine-inlet temperature, the effect of fuel-flow transients on engine dynamics was analyzed with respect to turbine-inlet temperature as the input. The speed responses of each spool to changes in turbine-inlet temperature were essentially identical and could be characterized as a first-order lag. Time constants decreased with increasing engine speed in a manner similar to the time-constant variation of a single-spool turbojet engine. Data obtained from an entirely different two-spool engine were also presented in order to determine the response to fuel flow and to permit greater generalization of results. It was found that the responses of both spools to a change in fuel flow again appeared to be identical first-order lags.

The response of engine variables to a change in exhaust-nozzle area at constant fuel flow was found to be more complicated than the response to turbine-inlet temperature or fuel flow. It was found that the outer-spool response appeared to approximate a first-order lag, but that the inner-spool response appeared to be higher order in the operating speed range. However, the magnitude of the inner-spool response was extremely small and consequently did not appreciably affect the apparent first-order response of the outer spool. At low speeds the magnitude of inner-spool speed changes increased and the response became first order.

As a general rule it appeared that engine dynamics were functions of inner-spool response for changes in turbine-inlet temperature (or fuel flow) and were functions of outer-spool response for changes in exhaust-nozzle area. Response to exhaust-nozzle area was faster than response to fuel flow or turbine-inlet temperature.

Experimentally determined responses of inner-spool speed to fuel flow and to turbine-inlet temperature and of both inner- and outer-spool speeds to exhaust-nozzle area were found to agree with analytically

derived equations of response. The conclusion that inner-spool time constant represents the basic engine response to fuel flow and turbine-inlet temperature was drawn from analysis.

Lewis Flight Propulsion Laboratory
National Advisory Committee for Aeronautics
Cleveland, Ohio, October 18, 1954

APPENDIX - DERIVATION OF RESPONSE EQUATIONS

The response of each spool to changes in the independent variables, turbine-inlet temperature and exhaust-nozzle area, is obtained from linearization of the functional relations:

$$q = q(N_o, N_i, T_4, A) \tag{A1}$$

$$Q = Q(N_o, N_i, T_4, A) \tag{A2}$$

Linear expansion of the functional relations around steady-state operating points gives

$$\Delta q = I_o \Delta \frac{dN_o}{dt} = I_o p \Delta N_o = q_{N_o} \Delta N_o + q_{N_i} \Delta N_i + q_{T_4} \Delta T_4 + q_A \Delta A \tag{A3}$$

$$\Delta Q = I_i \Delta \frac{dN_i}{dt} = I_i p \Delta N_i = Q_{N_o} \Delta N_o + Q_{N_i} \Delta N_i + Q_{T_4} \Delta T_4 + Q_A \Delta A \tag{A4}$$

By dividing equation (A3) by equation (A4) and eliminating either ΔN_i or ΔN_o, equations for the response of each spool can be obtained. At constant area, $\Delta A = 0$; and

$$\left| \frac{\Delta N_o}{\Delta T_4} \right|_A = \frac{q_{T_4}(I_i p - Q_{N_i}) + Q_{T_4} q_{N_i}}{(I_i p - Q_{N_i})(I_o p - q_{N_o}) - Q_{N_o} q_{N_i}} \tag{A5}$$

$$\left| \frac{\Delta N_i}{\Delta T_4} \right|_A = \frac{Q_{T_4}(I_o p - q_{N_o}) + Q_{N_o} q_{T_4}}{(I_i p - Q_{N_i})(I_o p - q_{N_o}) - Q_{N_o} q_{N_i}} \tag{A6}$$

Equations (A5) and (A6) can be rearranged as follows:

$$\left| \frac{\Delta N_o}{\Delta T_4} \right|_A = \frac{q_{T_4}}{q_{N_o}} \frac{\left(\frac{-I_i}{Q_{N_i}} p + 1 \right) + \frac{Q_{T_4} q_{N_i}}{Q_{N_i} q_{T_4}}}{\left(\frac{-I_i}{Q_{N_i}} p + 1 \right)\left(\frac{-I_o}{q_{N_o}} p + 1 \right) - \frac{Q_{N_o} q_{N_i}}{Q_{N_i} q_{N_o}}} \tag{A7}$$

$$\left|\frac{\Delta N_i}{\Delta T_4}\right|_A = \frac{Q_{T_4}}{Q_{N_i}} \frac{\left(\frac{-I_o}{q_{N_o}} p + 1\right) + \frac{Q_{N_o} q_{T_4}}{q_{N_o} Q_{T_4}}}{\left(\frac{-I_i}{Q_{N_i}} p + 1\right)\left(\frac{-I_o}{q_{N_o}} p + 1\right) - \frac{Q_{N_o} q_{N_i}}{Q_{N_i} q_{N_o}}} \tag{A8}$$

Let $\tau_o = \frac{-I_o}{q_{N_o}}$ and $\tau_i = \frac{-I_i}{Q_{N_i}}$; then,

$$\left|\frac{\Delta N_o}{\Delta T_4}\right|_A = \frac{q_{T_4}}{q_{N_o}} \frac{(\tau_i p + 1) + Q_{T_4} q_{N_i}}{(\tau_i p + 1)(\tau_o p + 1) - \frac{Q_{N_o} q_{N_i}}{Q_{N_i} q_{N_o}}} \tag{A9}$$

$$\left|\frac{\Delta N_i}{\Delta T_4}\right|_A = \frac{Q_{T_4}}{Q_{N_i}} \frac{(\tau_o p + 1) + \frac{Q_{N_o} q_{T_4}}{q_{N_o} Q_{T_4}}}{(\tau_i p + 1)(\tau_o p + 1) - \frac{Q_{N_o} q_{N_i}}{Q_{N_i} q_{N_o}}} \tag{A10}$$

If equations (A3) and (A4) are used to determine response to exhaust-nozzle area at constant turbine-inlet temperature ($\Delta T_4 = 0$), then the following equations are obtained in a manner similar to the preceding development:

$$\left|\frac{\Delta N_o}{\Delta A}\right|_{T_4} = \frac{q_A}{q_{N_o}} \frac{(\tau_i p + 1) + \frac{Q_A q_{N_i}}{Q_{N_i} q_A}}{(\tau_i p + 1)(\tau_o p + 1) - \frac{Q_{N_o} q_{N_i}}{Q_{N_i} q_{N_o}}} \tag{A11}$$

$$\left|\frac{\Delta N_i}{\Delta A}\right|_{T_4} = \frac{Q_A}{Q_{N_i}} \frac{(\tau_o p + 1) + \frac{Q_{N_o} q_A}{Q_{N_i} q_{N_o}}}{(\tau_i p + 1)(\tau_o p + 1) - \frac{Q_{N_o} q_{N_i}}{Q_{N_i} q_{N_o}}} \tag{A12}$$

Evaluation of the partial derivatives on the basis of thermodynamic engine relations near rated-speed conditions indicates that the quantities $\frac{Q_{N_o} q_{N_i}}{Q_{N_i} q_{N_o}}$ and $\frac{Q_{N_o} q_{T_4}}{q_{N_o} Q_{T_4}}$ are negligible, the quantity Q_A is equal to zero, and the quantity $\frac{Q_{N_o} q_A}{Q_{N_i} q_{N_o}}$ is very small.

The equations of response for a two-spool engine near rated speed are therefore approximated by the following equations:

$$\left|\frac{\Delta N_o}{\Delta T_4}\right|_A = \frac{q_{T_4}}{q_{N_o}} \frac{(\tau_i p + 1) + \frac{Q_{T_4} q_{N_i}}{Q_{N_i} q_{T_4}}}{(\tau_i p + 1)(\tau_o p + 1)} \tag{A13}$$

$$\left|\frac{\Delta N_i}{\Delta T_4}\right|_A = \frac{Q_{T_4}}{Q_{N_i}} \frac{1}{\tau_i p + 1} \tag{A14}$$

$$\left|\frac{\Delta N_o}{\Delta A}\right|_{T_4} = \frac{q_A}{q_{N_o}} \frac{1}{\tau_o p + 1} \tag{A15}$$

$$\left|\frac{\Delta N_i}{\Delta A}\right|_{T_4} = \frac{\frac{Q_{N_o} q_A}{Q_{N_i} q_{N_o}}}{(\tau_i p + 1)(\tau_o p + 1)} \cong 0 \tag{A16}$$

REFERENCES

1. Gold, Harold, and Otto, Edward W.: An Analytical and Experimental Study of the Transient Response of a Pressure-Regulating Relief Valve in a Hydraulic Circuit. NACA TN 3102, 1954.

2. Delio, Gene J.: Evaluation of Three Methods for Determining Dynamic Characteristics of a Turbojet Engine. NACA TN 2634, 1952.

TABLE I. - FREQUENCIES CORRESPONDING TO POINTS SHOWN ON FREQUENCY-RESPONSE CURVES

Point	Frequencies applicable for figs. —		
	8, 11, 12, 21, 22	9, 13, 23	24
A	0.1047	0.05236	0.0262
B	.131	.06545	.0327
C	.157	.07854	.03295
D	.2094	.1047	.05325
E	.262	.1309	.0654
F	.314	.1571	.0785
G	.419	.2094	.1047
H	.523	.2618	.131
I	.628	.3142	.157
J	.873	.4363	.218
K	1.047	.5263	.262
L	1.31	.6545	.327
M	1.57	.7854	.3295
N	2.094	1.047	.5235
O	2.62	1.309	.654
P	3.14	1.571	.785
Q	4.19	2.094	1.047
R	5.23	2.618	1.31
S	6.28	3.142	1.57
T	8.73	4.363	2.18
U	10.47	5.236	2.62
V	13.11	6.545	3.27
W	15.71	7.854	3.925
X	20.94	10.47	5.235

TABLE II. - ENGINE TRANSFER FUNCTIONS

Response of engine variable	To change in independent variable	With other independent variable held constant	Gives approximate transfer function
N_o	W_f	A	$\left\|\frac{\Delta N_o}{\Delta W_f}\right\|_A = K\frac{1}{1+\tau_1' p}$ $\tau_1' = \frac{-I_1}{Q'_{N_1}}$
N_o	T_4	A	$\left\|\frac{\Delta N_o}{\Delta T_4}\right\|_A = K\frac{1}{1+\tau_1 p}$ $\tau_1 = \frac{-I_1}{Q_{N_1}} \approx 0.65$ sec (near rated speed)
N_o	A	W_f	$\left\|\frac{\Delta N_o}{\Delta A}\right\|_{W_f} = K\frac{1}{1+\tau_o' p}$ $\tau_o' = \frac{-I_o}{q'_{N_o}} \approx 0.45$ sec (near rated speed)
N_1	W_f	A	$\left\|\frac{\Delta N_1}{\Delta W_f}\right\|_A = K\frac{1}{1+\tau_1' p}$ $\tau_1' = \frac{-I_1}{Q'_{N_1}}$
N_1	T_4	A	$\left\|\frac{\Delta N_1}{\Delta T_4}\right\|_A = K\frac{1}{1+\tau_1 p}$ $\tau_1 = \frac{-I_1}{Q_{N_1}} \approx 0.65$ sec (near rated speed)
N_1 at medium and high speed	A	W_f	$\left\|\frac{\Delta N_1}{\Delta A}\right\|_{W_f} \approx 0$ (ΔN_1 has small amplitude, second order, and negative change near rated speed)
P_2	T_4	A	$\left\|\frac{\Delta P_2}{\Delta T_4}\right\|_A = K\frac{(1+a\tau_1 p)}{1+\tau_1 p}$ a = rise ratio $\approx$ 0.13 near rated speed a = 0 below 75 percent rated N_1 $\tau_1 = \frac{-I_1}{Q_{N_1}} \approx 0.65$ sec (near rated speed)
P_2	A	W_f	$\left\|\frac{\Delta P_2}{\Delta A}\right\|_{W_f} \approx K\frac{1}{1+\tau_o' p}$ $\tau_o' = \frac{-I_o}{q'_{N_o}} \approx 0.45$ sec (near rated speed)
T_2	T_4	A	$\left\|\frac{\Delta T_2}{\Delta T_4}\right\|_A = K\frac{(1+a\tau_1 p)}{1+\tau_1 p}$ a = rise ratio $\approx$ 0.1 near rated speed a = 0 below 75 percent rated N_1 $\tau_1 = \frac{-I_1}{Q_{N_1}} \approx 0.65$ sec (near rated speed)
T_2	A	W_f	$\left\|\frac{\Delta T_2}{\Delta A}\right\|_{W_f} = K\frac{1}{1+\tau_o' p}$ $\tau_o' = \frac{-I_o}{q'_{N_o}} \approx 0.45$ sec (near rated speed)
P_3	T_4	A	$\left\|\frac{\Delta P_3}{\Delta T_4}\right\|_A = K\frac{(1+a\tau_1 p)}{1+\tau_1 p}$ a = rise ratio $\approx$ 0.35 near rated speed $\tau_1 = \frac{-I_1}{Q_{N_1}} \approx 0.65$ sec (near rated speed)
P_3	A	W_f	$\left\|\frac{\Delta P_3}{\Delta A}\right\|_{W_f} = K\frac{1}{1+\tau_o' p}$ $\tau_o' = \frac{-I_o}{q'_{N_o}} \approx 0.45$ sec (near rated speed)
T_3	T_4	A	$\left\|\frac{\Delta T_3}{\Delta T_4}\right\|_A = K\frac{(1+a\tau_1 p)}{1+\tau_1 p}$ a = rise ratio $\approx$ 0.13 near rated speed $\tau_1 = \frac{-I_1}{Q_{N_1}} \approx 0.65$ sec (near rated speed)
T_3	A	W_f	$\left\|\frac{\Delta T_3}{\Delta A}\right\|_{W_f} = K\frac{1}{1+\tau_o' p}$ $\tau_o' = \frac{-I_o}{q'_{N_o}} \approx 0.45$ sec (near rated speed)
T_4	A	W_f	$\left\|\frac{\Delta T_4}{\Delta A}\right\|_{W_f} = K\frac{(1+a\tau_o' p)}{1+\tau_o' p}$ a = rise ratio $\approx$ 0.1 near rated speed $\tau_o' = \frac{-I_o}{q'_{N_o}} \approx 0.45$ sec (near rated speed)
P_9	T_4	A	$\left\|\frac{\Delta P_9}{\Delta T_4}\right\|_A = K\frac{(1+a\tau_1 p)}{1+\tau_1 p}$ a = rise ratio $\approx$ 0.03 near rated speed $\tau_1 = \frac{-I_1}{Q_{N_1}} \approx 0.65$ sec (near rated speed)
P_9	A	W_f	$\left\|\frac{\Delta P_9}{\Delta A}\right\|_{W_f} = K\frac{(1+a\tau_o' p)}{1+\tau_o' p}$ a = rise ratio $\approx$ 1.5 near rated speed $\tau_o' = \frac{-I_o}{q'_{N_o}} \approx 0.65$ sec (near rated speed)
T_9	T_4	A	$\left\|\frac{\Delta T_9}{\Delta T_4}\right\|_A = K$ (near rated speed)
T_9	A	W_f	$\left\|\frac{\Delta T_9}{\Delta A}\right\|_{W_f} = K\frac{(1+a\tau_o' p)}{1+\tau_o' p}$ a = rise ratio $\approx$ 0.1 near rated speed $\tau_o' = \frac{-I_o}{q'_{N_o}} \approx 0.45$ sec (near rated speed)
F	T_4	A	$\left\|\frac{\Delta F}{\Delta T_4}\right\|_A = K\frac{(1+a\tau_1 p)}{1+\tau_1 p}$ a = rise ratio $\approx$ 0.45 near rated speed $\tau_1 = \frac{-I_1}{Q_{N_1}} \approx 0.65$ sec (near rated speed)
F in upper-speed range	A	W_f	$\left\|\frac{\Delta F}{\Delta A}\right\|_{W_f} = K\frac{(1+a\tau_o' p)}{1+\tau_o' p}$ a = rise ratio $\approx$ -30 near rated speed for area closing $\tau_o' = \frac{-I_o}{q'_{N_o}} \approx 0.45$ sec (near rated speed) Note: Steady-state gain $K \approx 0$

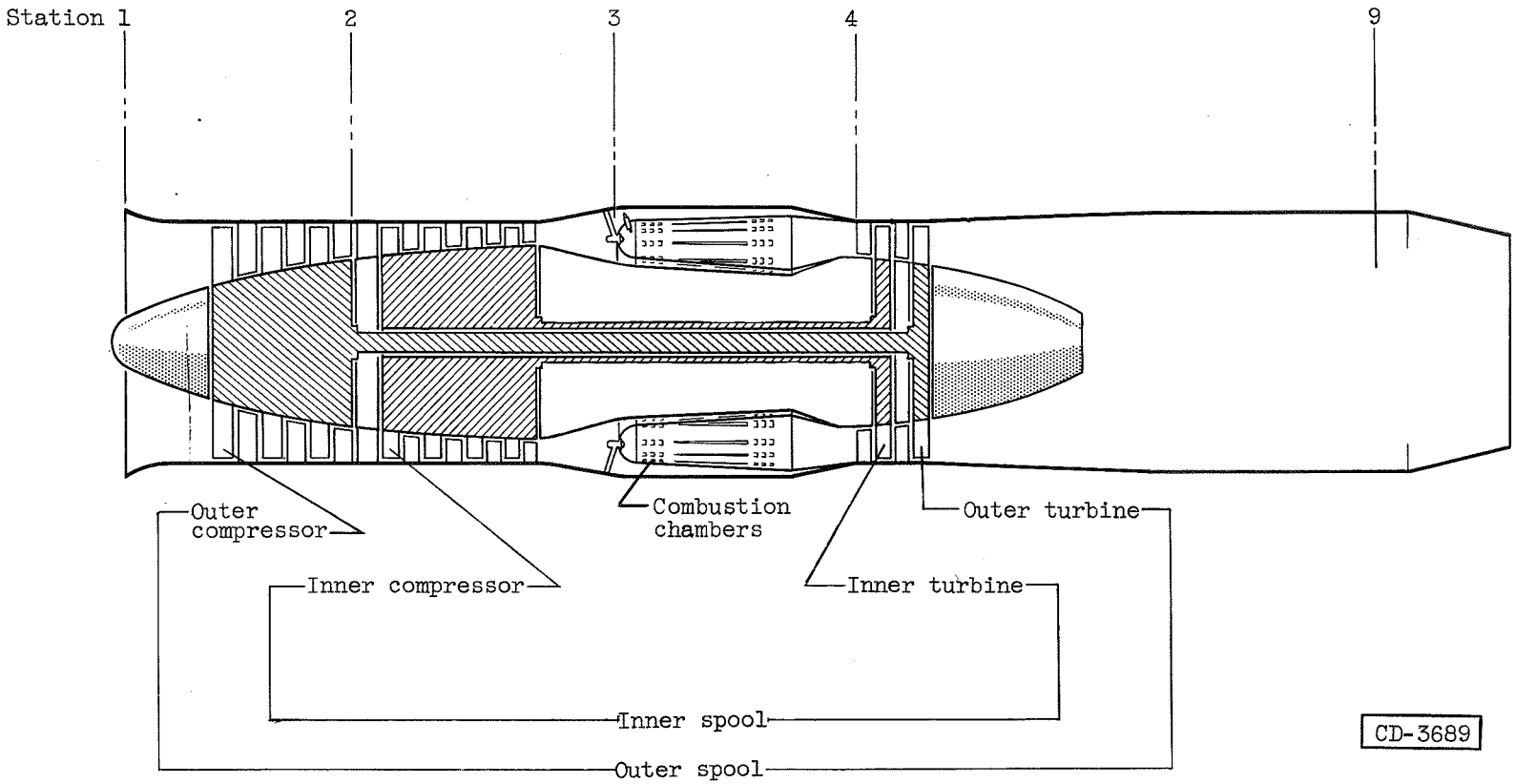

Figure 1. - Schematic of two-spool engine and instrumentation stations.

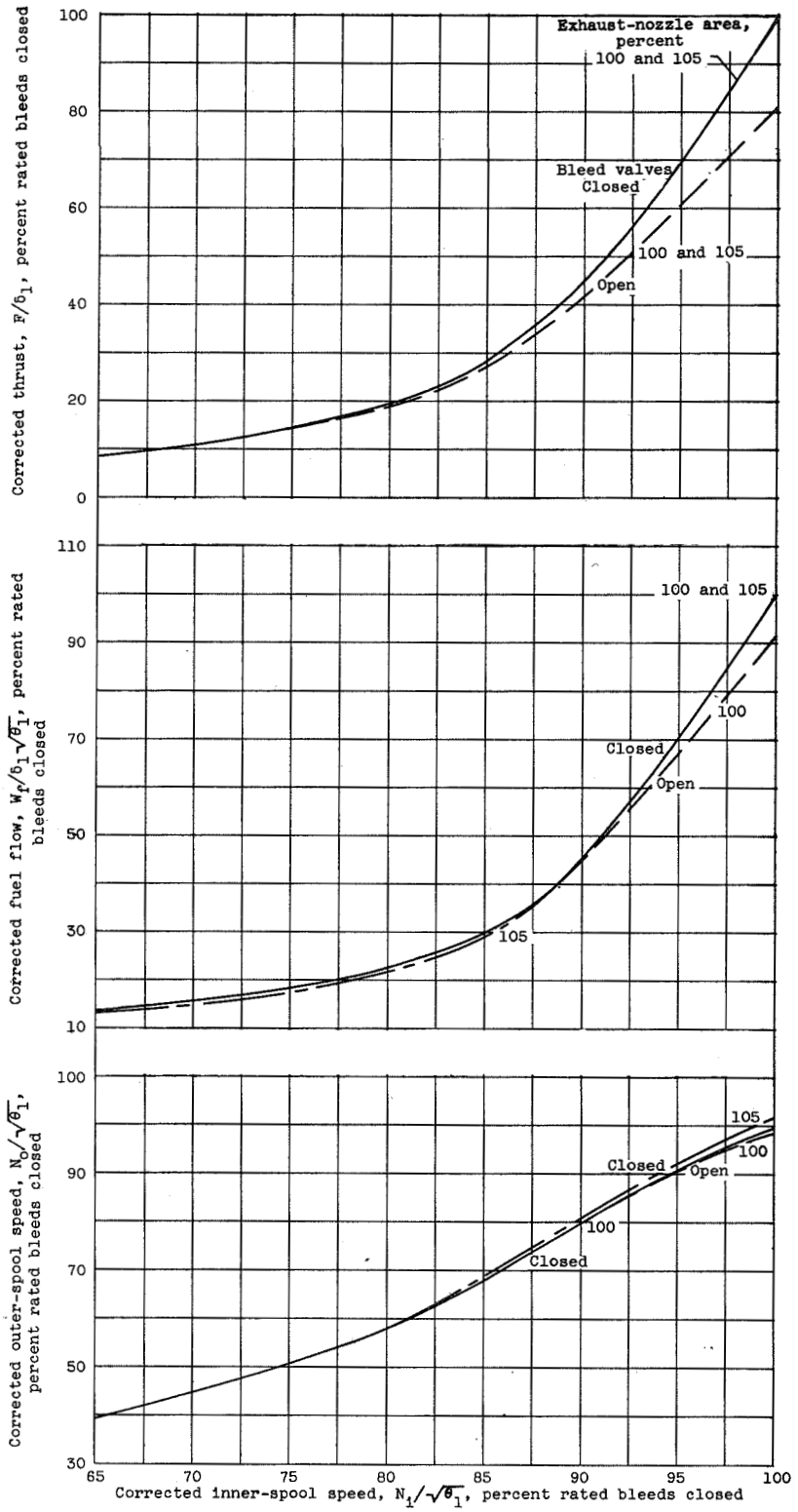

(a) Outer-spool speed, fuel flow, and thrust.

Figure 2. - Steady-state performance of two-spool turbojet engine.

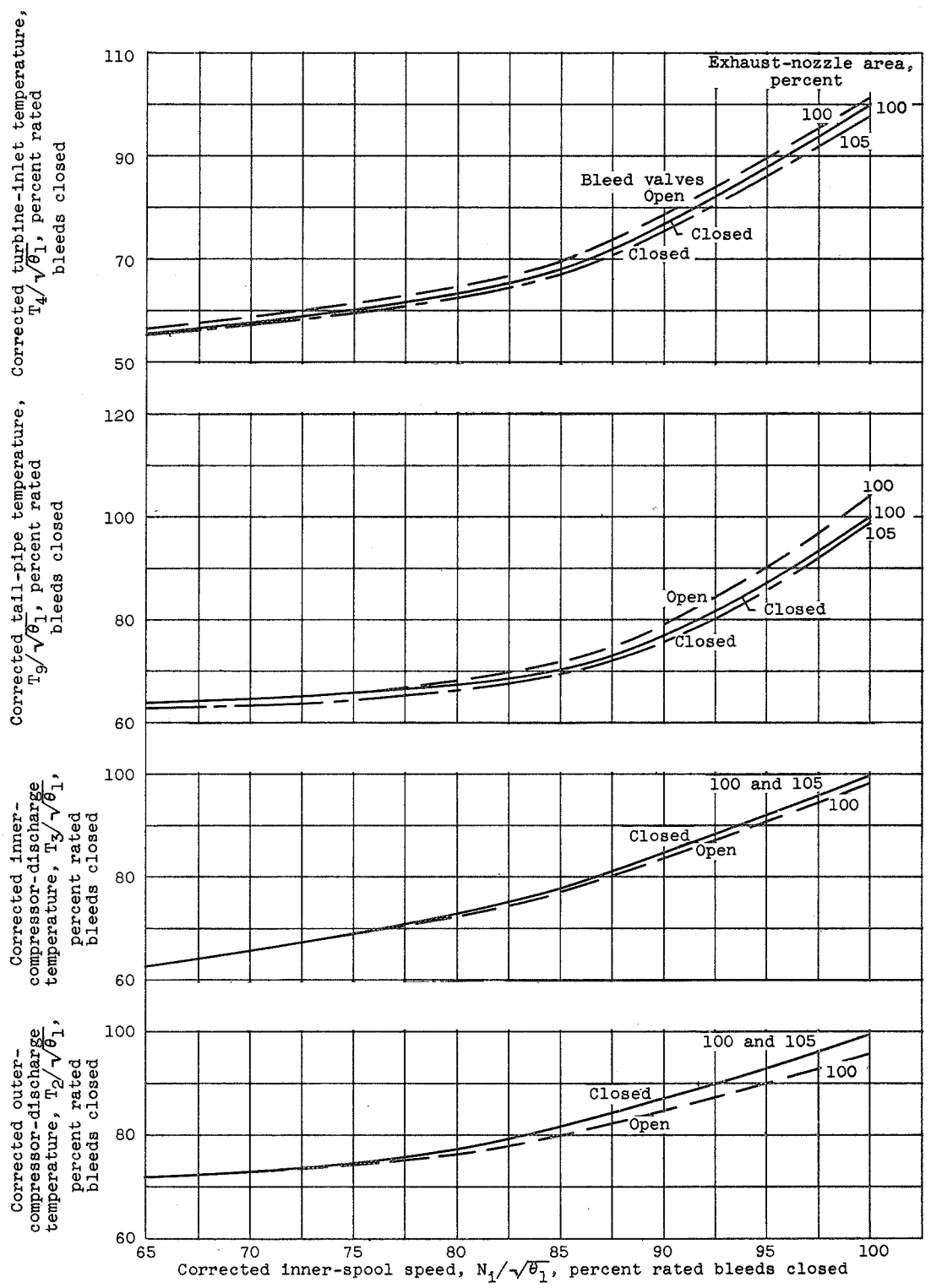

(b) Temperatures.

Figure 2. - Continued. Steady-state performance of two-spool turbojet engine.

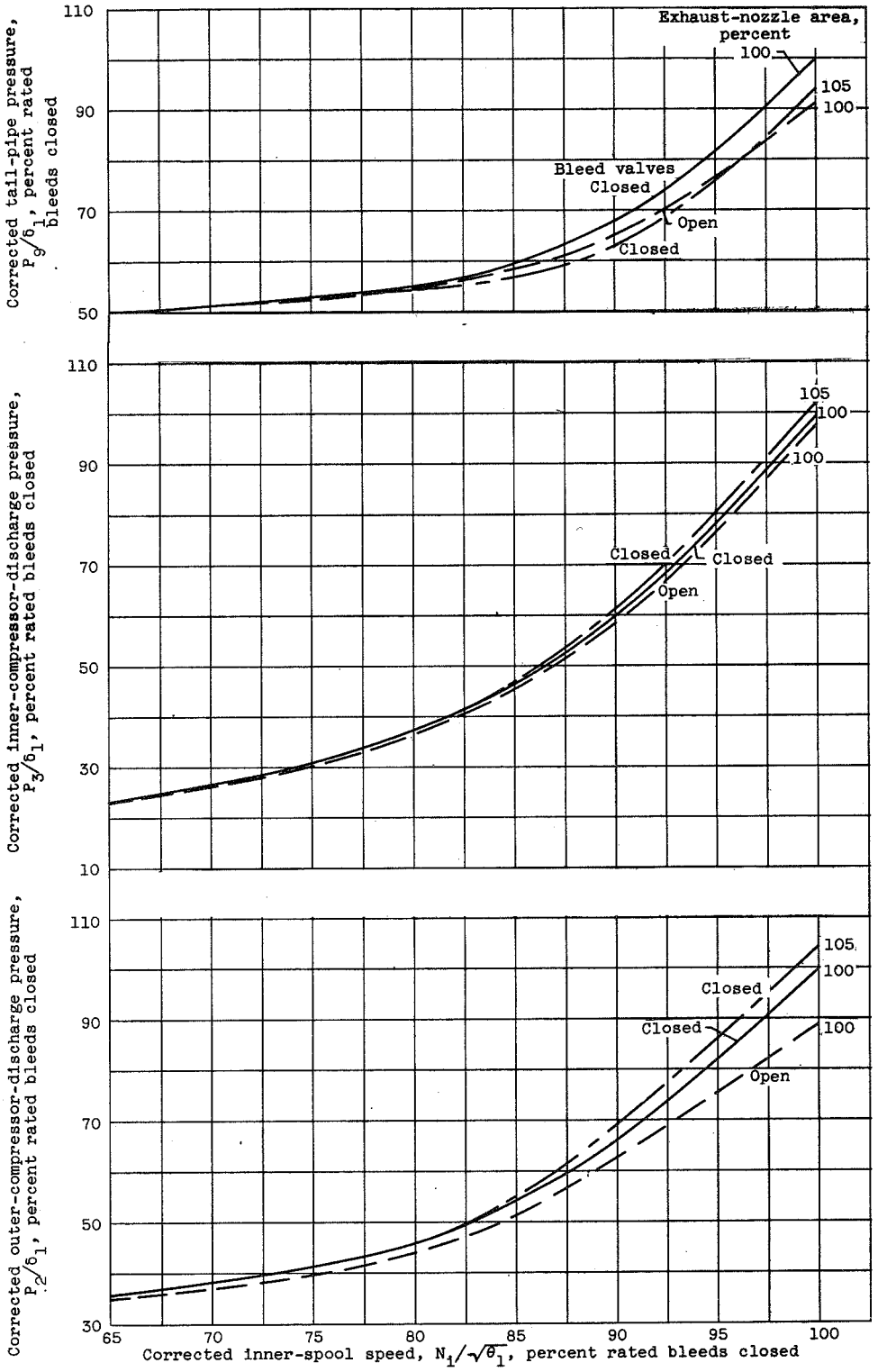

(c) Pressures.

Figure 2. - Concluded. Steady-state performance of two-spool turbojet engine.

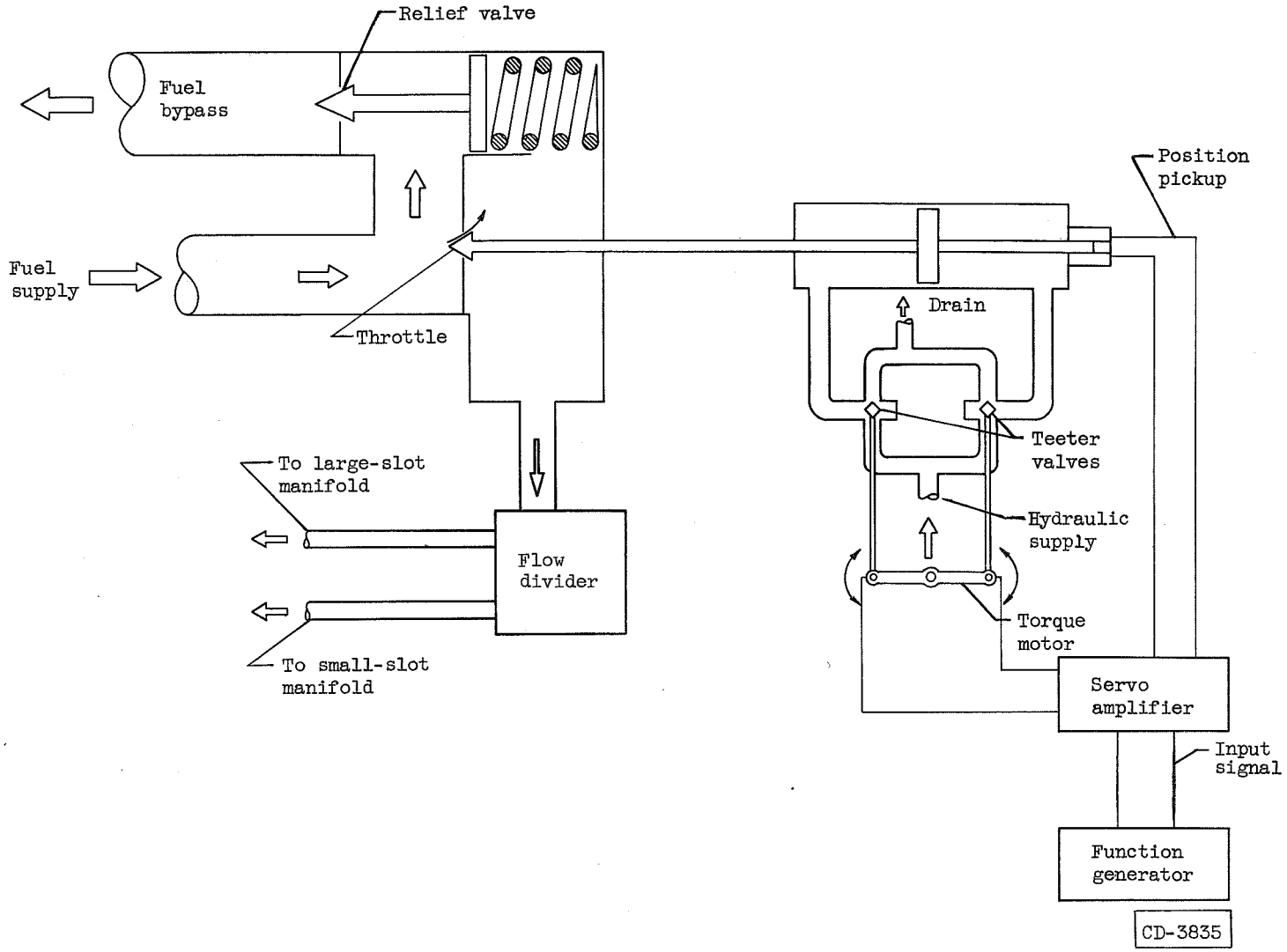

Figure 3. - Fuel system.

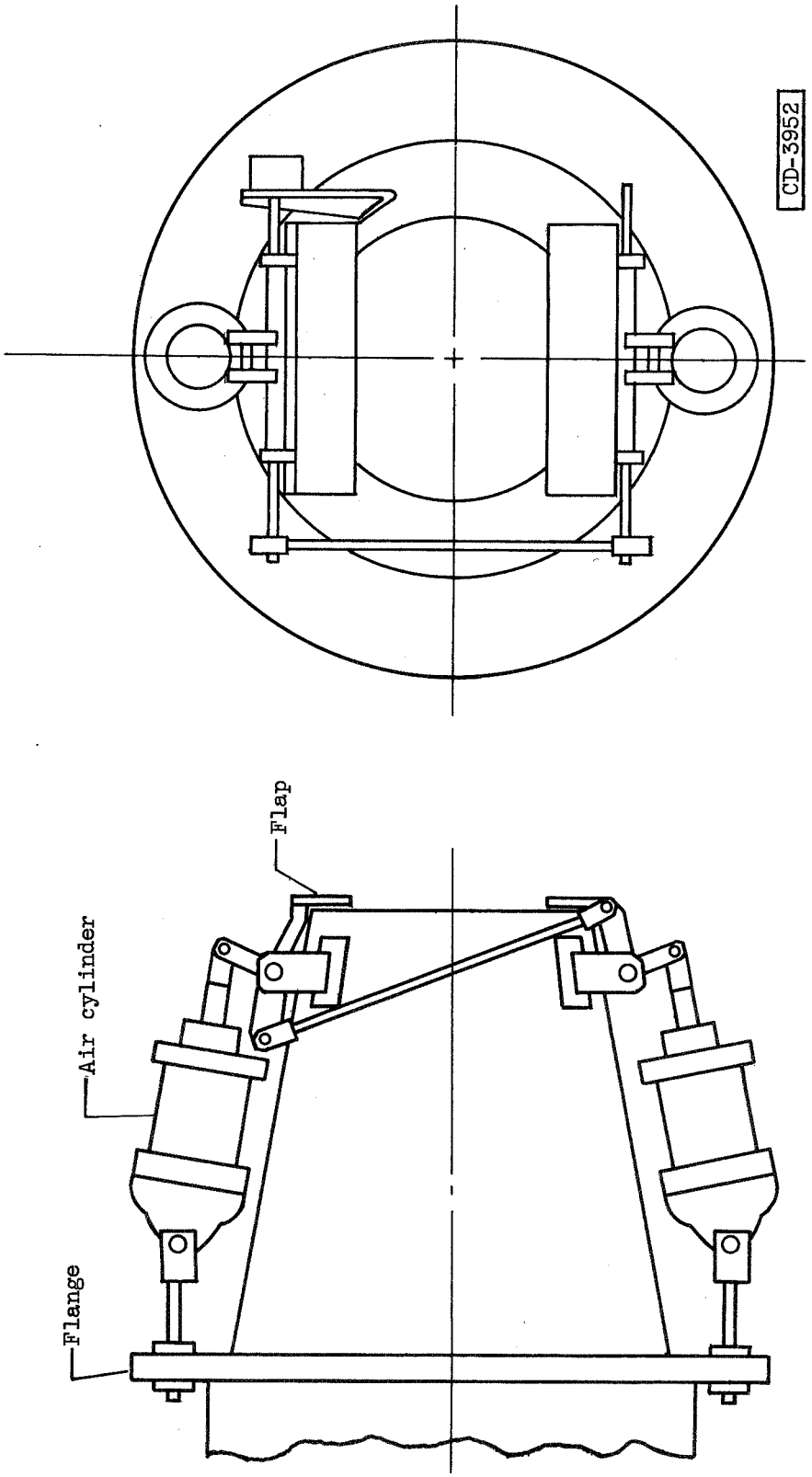

Figure 4. - Variable-area exhaust nozzle.

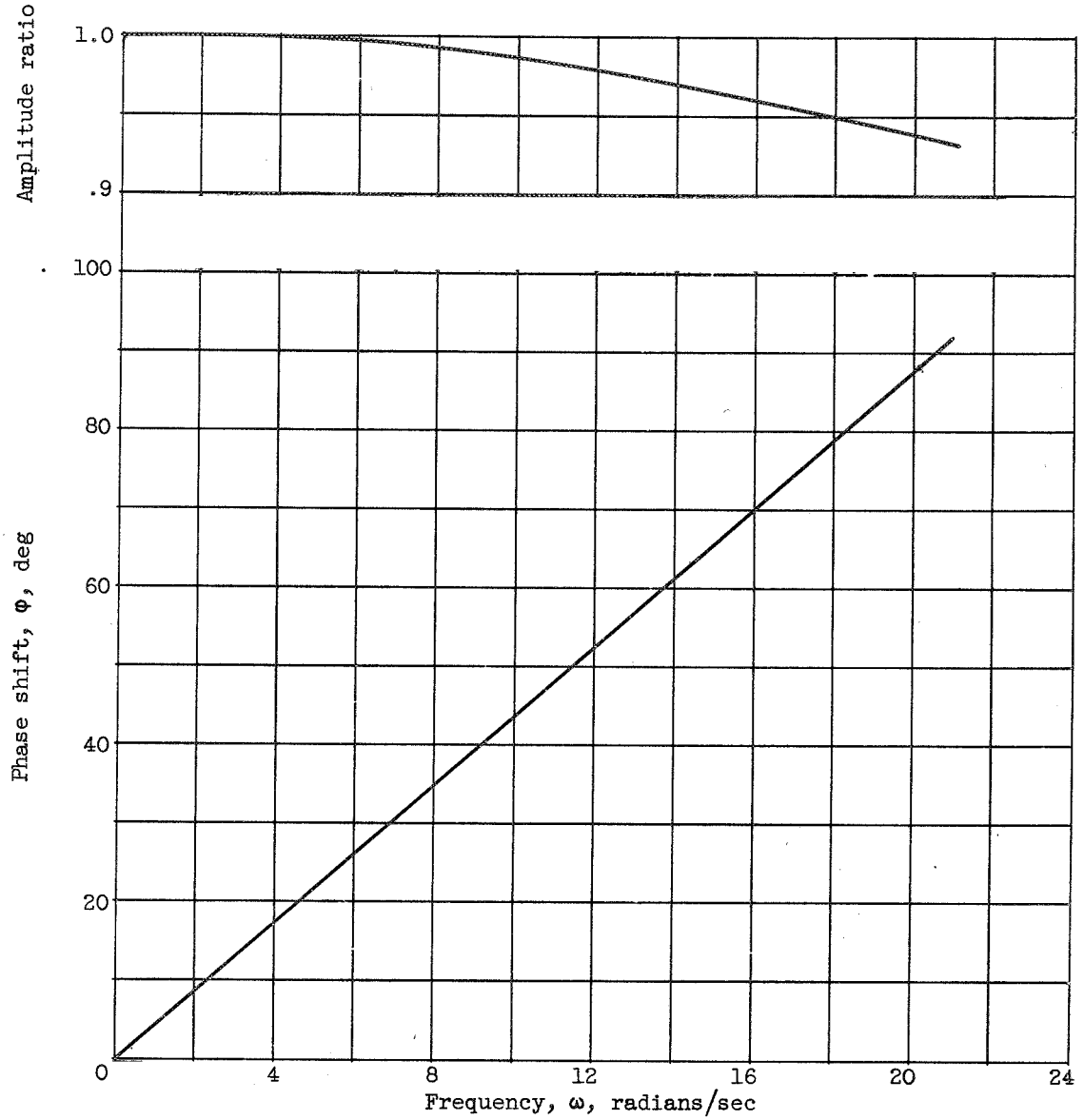

Figure 5. - Characteristic filters used on engine-speed measurements.

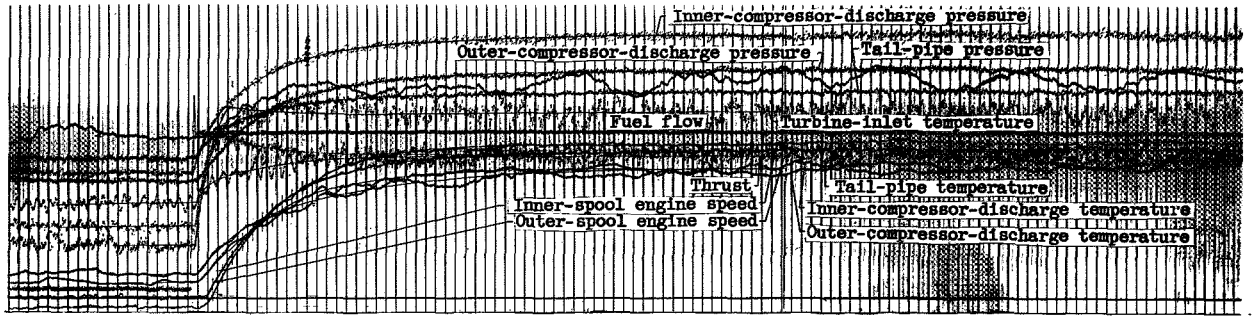

(a) Corrected outer-spool speed range, 87.5 to 92.9 percent rated; corrected inner-spool speed range, 93.5 to 96.1 percent rated; bleed valves closed.

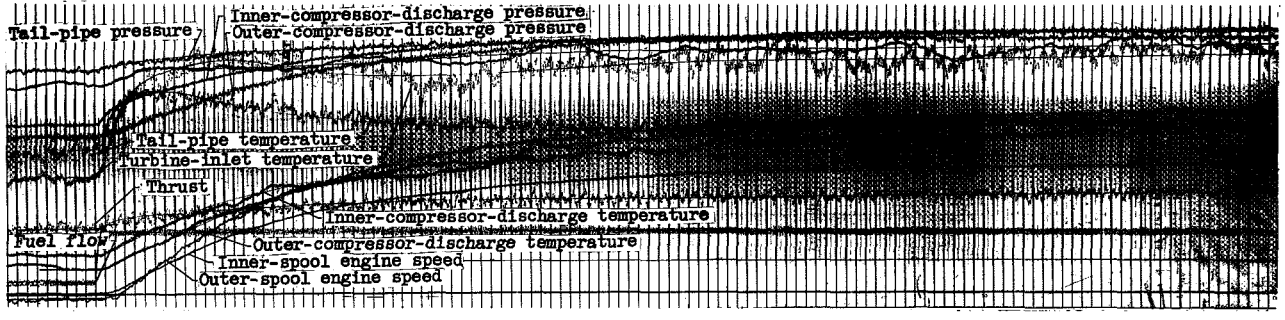

(b) Corrected outer-spool speed range, 57.6 to 62.9 percent rated; corrected inner-spool speed range, 79.6 to 82.5 percent rated; bleed valves open.

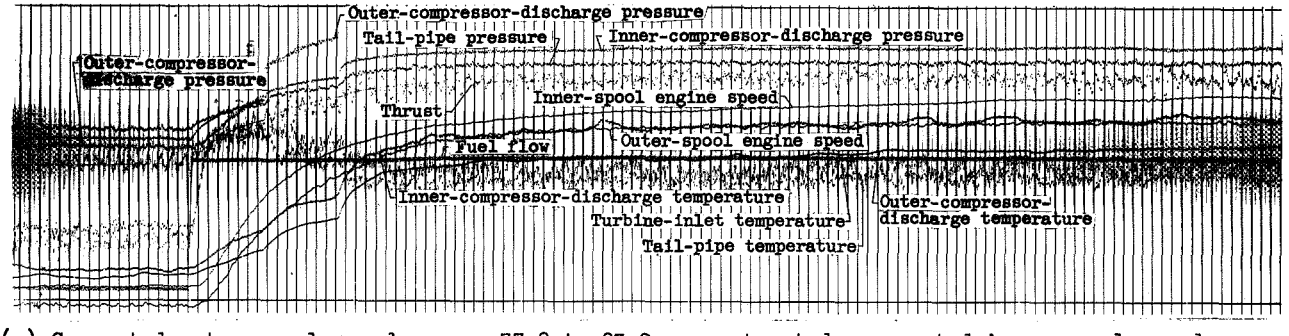

(c) Corrected outer-spool speed range, 77.8 to 83.9 percent rated; corrected inner-spool speed range, 88.7 to 91.3 percent rated; bleed valves closed during transient.

Figure 6. - Response of engine variables to step in fuel flow.

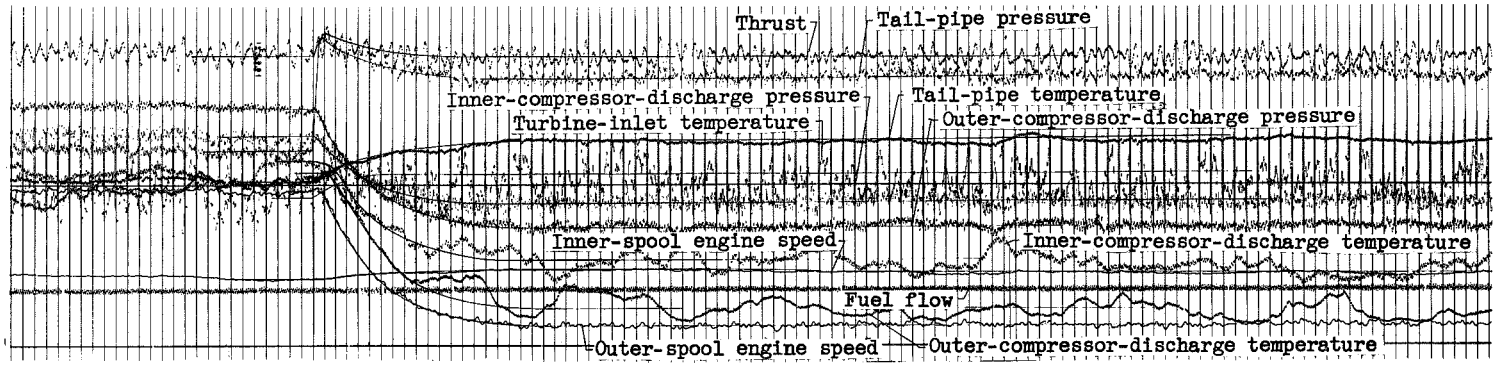

(a) Corrected outer-spool speed range, 95.9 to 92.9 percent rated; corrected inner-spool speed range, 96.6 to 96.7 percent rated; bleed valves closed.

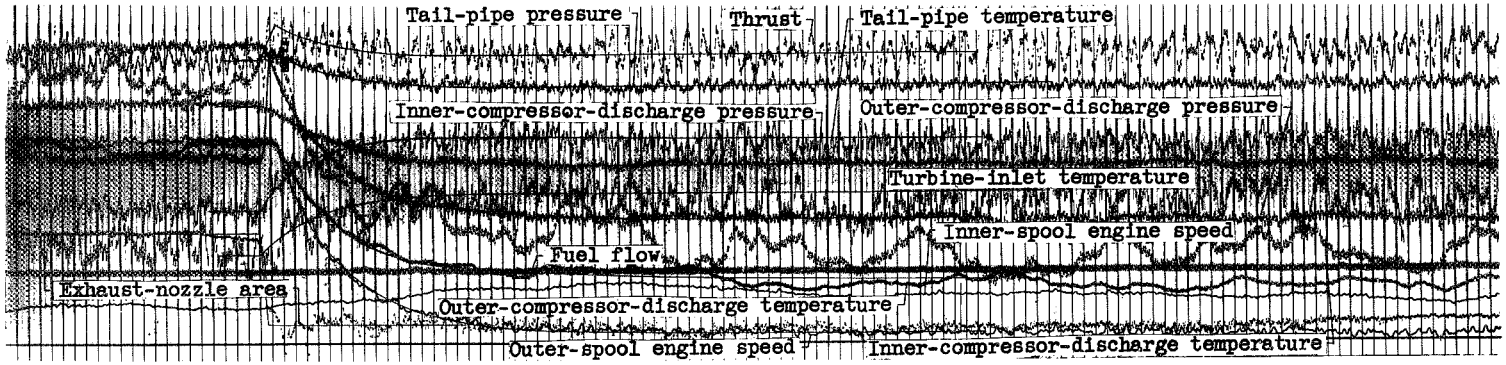

(b) Corrected outer-spool speed range, 88.0 to 85.1 percent rated; corrected inner-spool speed range, 92.9 to 93.0 percent rated; bleed valves closed.

Figure 7. - Response of engine variables to change in exhaust-nozzle area.

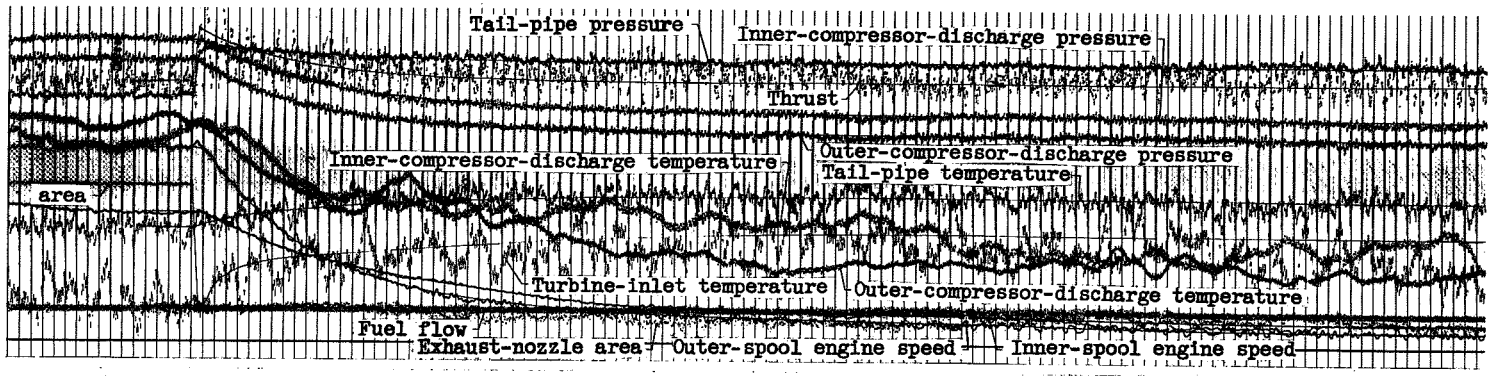

(c) Corrected outer-spool speed range, 65.9 to 63.1 percent rated; corrected inner-spool speed range, 83.8 to 83.1 percent rated; bleed valves open.

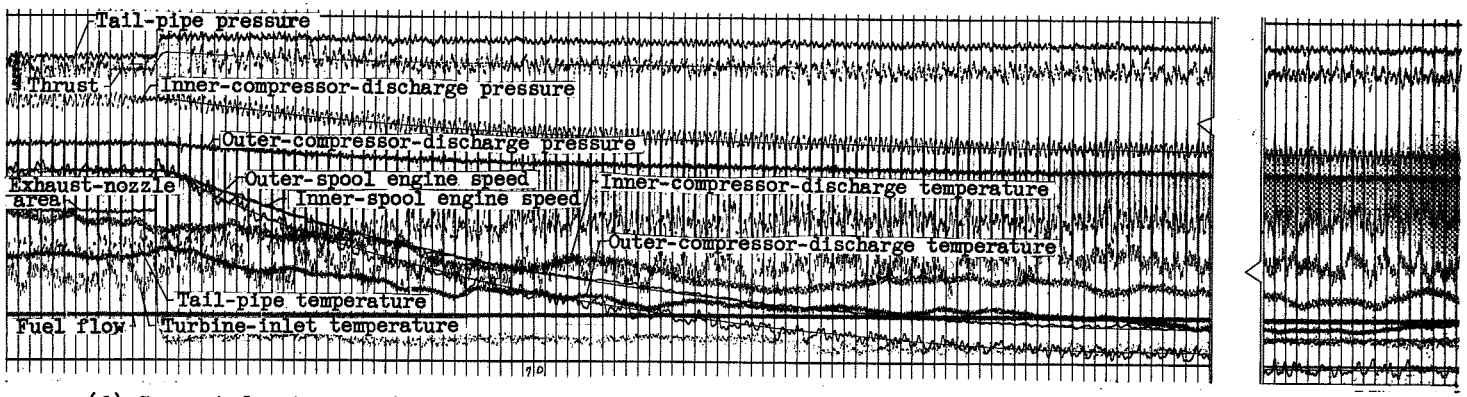

(d) Corrected outer-spool speed range, 46.4 to 44.7 percent rated; corrected inner-spool speed range, 71.5 to 70.0 percent rated; bleed valves open.

Figure 7. - Concluded. Response of engine variables to change in exhaust-nozzle area.

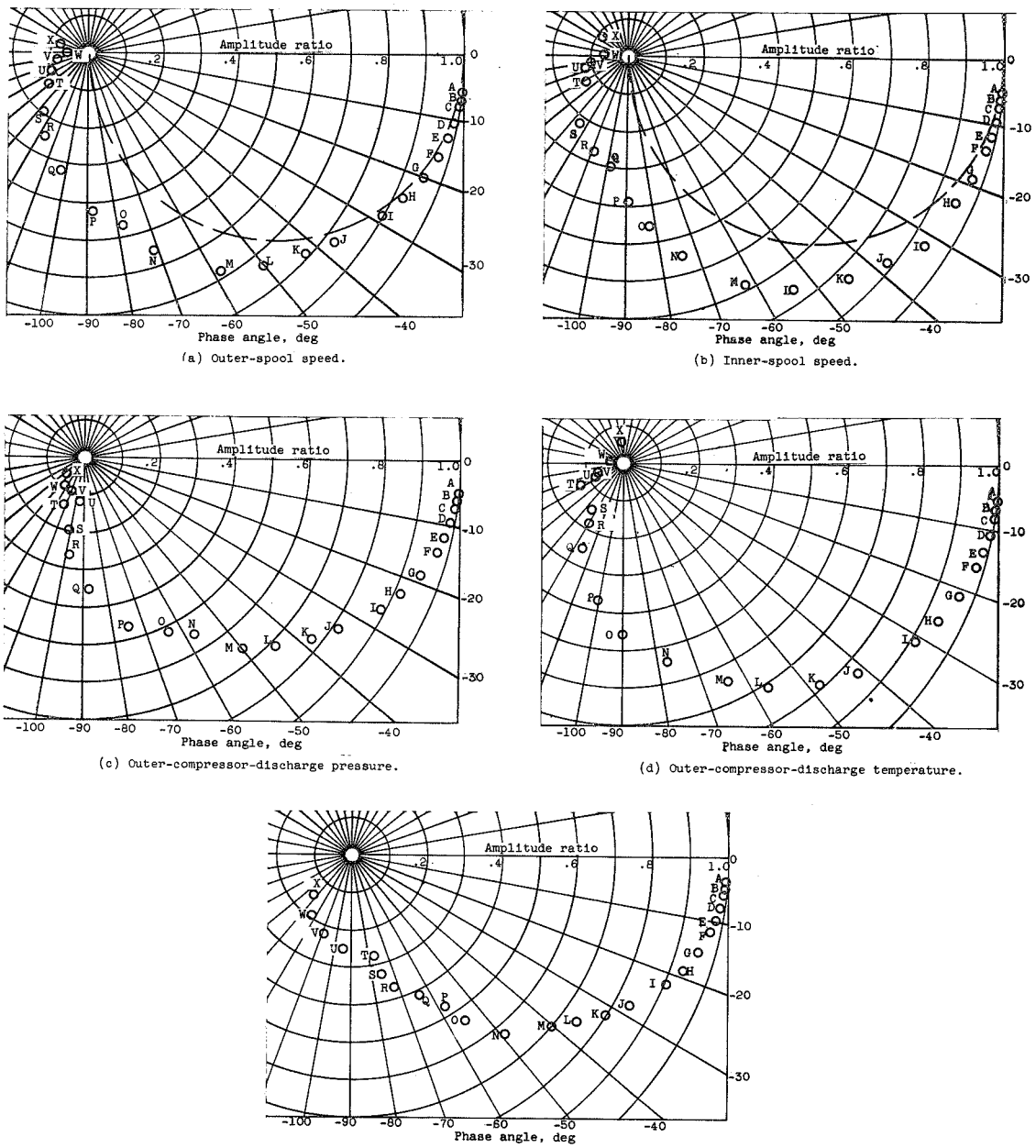

(a) Outer-spool speed.

(b) Inner-spool speed.

(c) Outer-compressor-discharge pressure.

(d) Outer-compressor-discharge temperature.

(e) Inner-compressor-discharge pressure.

Figure 8. - Frequency response of engine variables to change in fuel flow for increase in corrected outer-spool speed from 93.5 to 96.1 percent rated and increase in corrected inner-spool speed from 87.5 to 92.9 percent rated. Bleed valves closed.

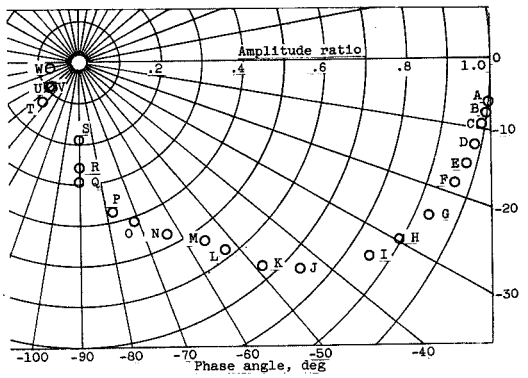

(f) Inner-compressor-discharge temperature.

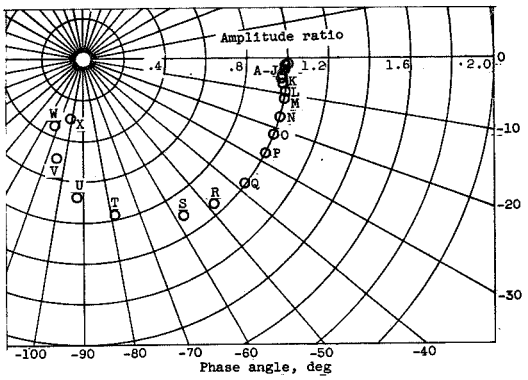

(g) Turbine-inlet temperature.

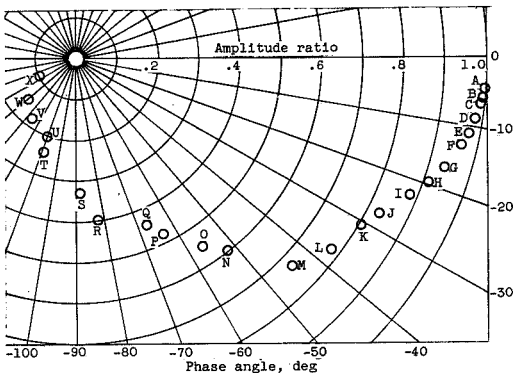

(h) Tail-pipe pressure.

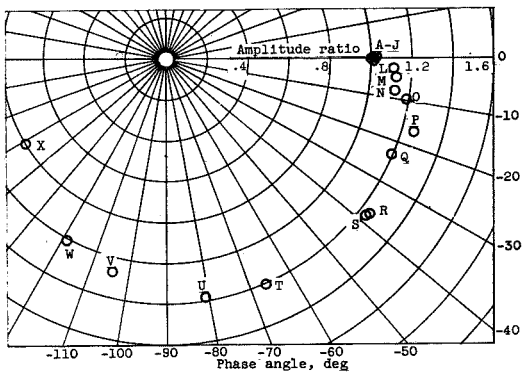

(i) Tail-pipe temperature.

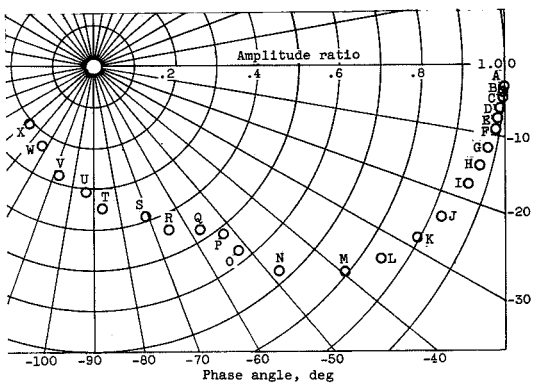

(j) Thrust.

Figure 8. - Concluded. Frequency response of engine variables to change in fuel flow for increase in corrected outer-spool speed from 93.5 to 96.1 percent rated and increase in corrected inner-spool speed from 87.5 to 92.9 percent rated. Bleed valves closed.

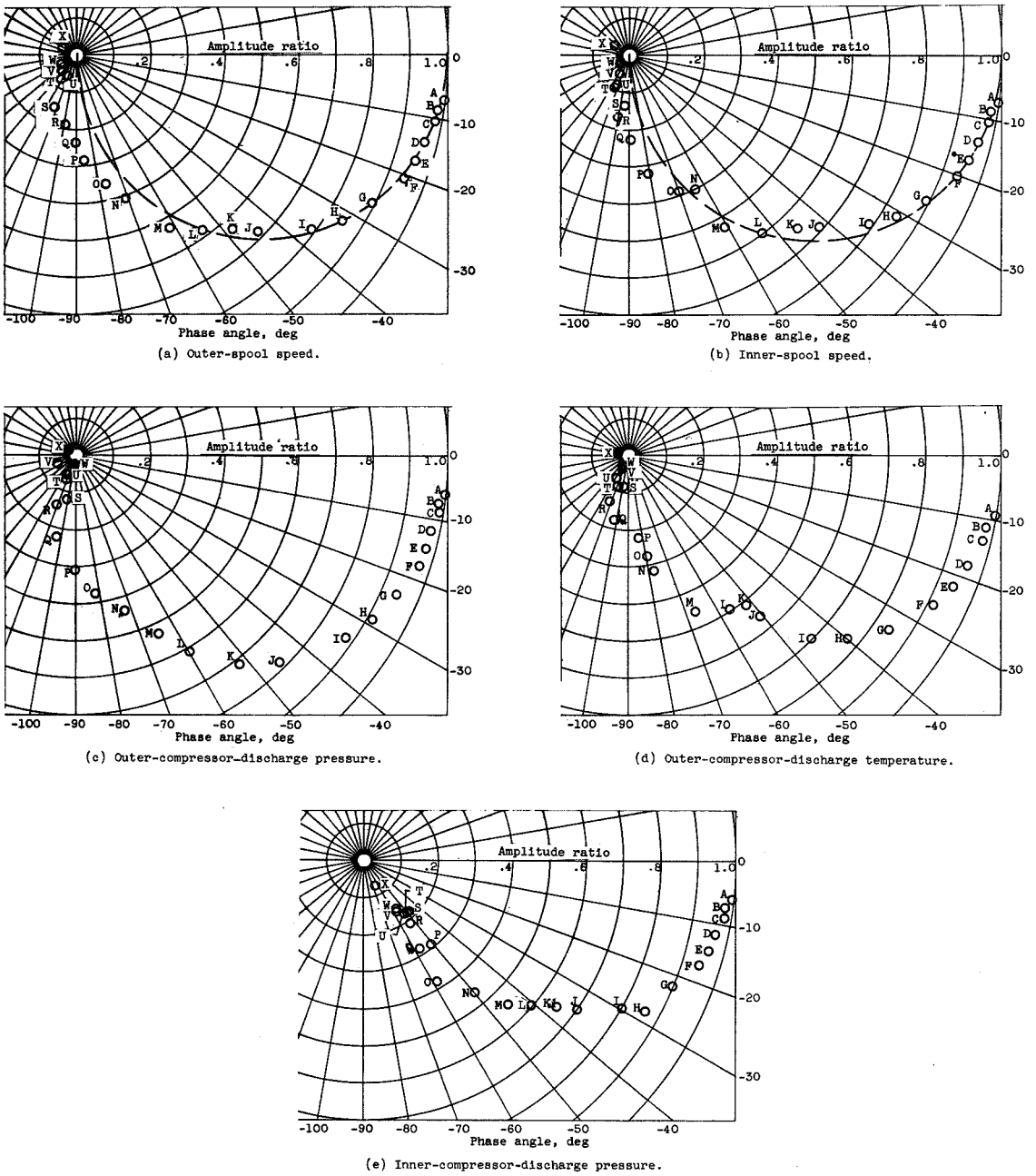

(a) Outer-spool speed.

(b) Inner-spool speed.

(c) Outer-compressor-discharge pressure.

(d) Outer-compressor-discharge temperature.

(e) Inner-compressor-discharge pressure.

Figure 9. - Frequency response of engine variables to change in fuel flow for increase in corrected outer-spool speed from 79.6 to 82.5 percent rated and increase in corrected inner-spool speed from 57.6 to 62.9 percent rated. Bleed valves open.

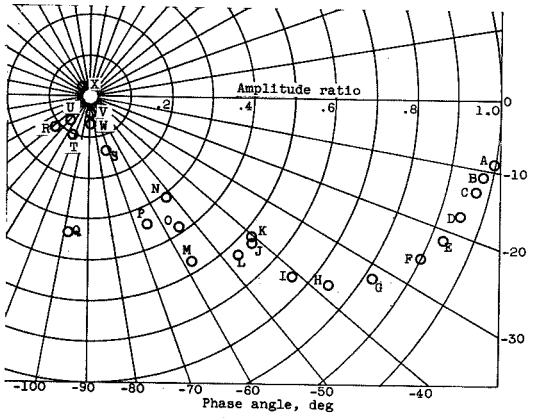

(f) Inner-compressor-discharge temperature.

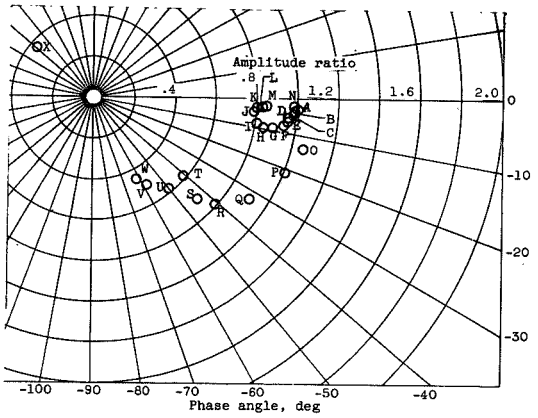

(g) Turbine-inlet temperature.

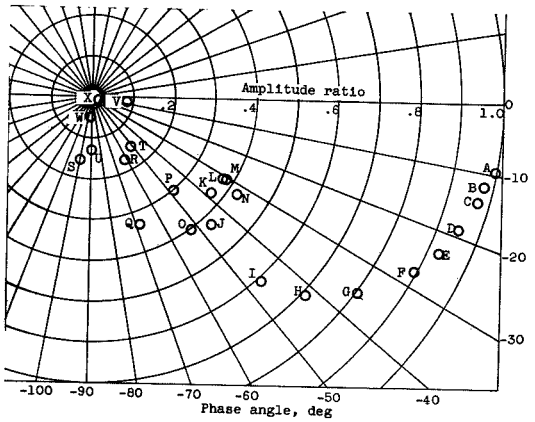

(h) Tail-pipe pressure.

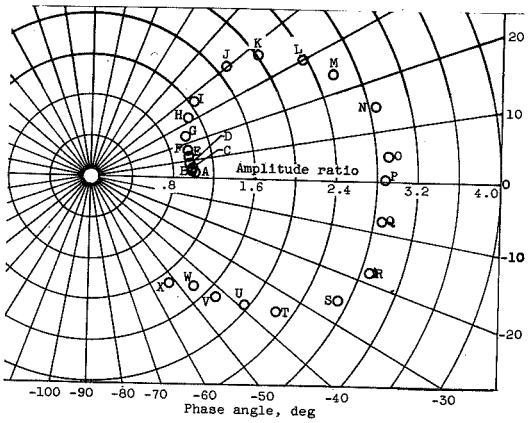

(i) Tail-pipe temperature.

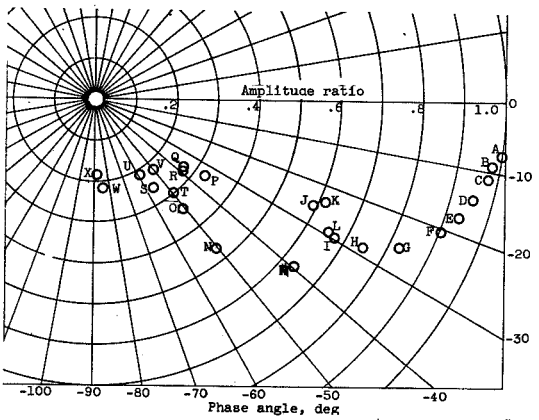

(j) Thrust.

Figure 9. - Concluded. Frequency response of engine variables to change in fuel flow for increase in corrected outer-spool speed from 79.6 to 82.5 percent rated and increase in corrected inner-spool speed from 57.6 to 62.9 percent rated. Bleed valves open.

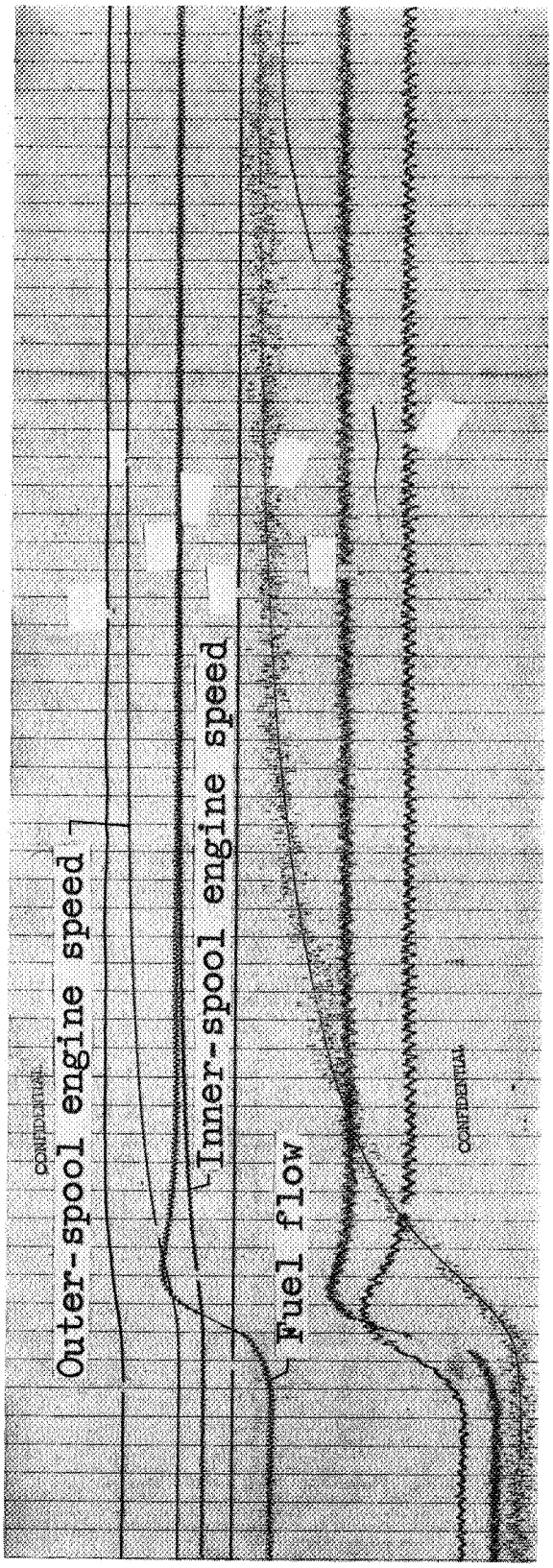

Figure 10. - Transient data from engine of different manufacture.

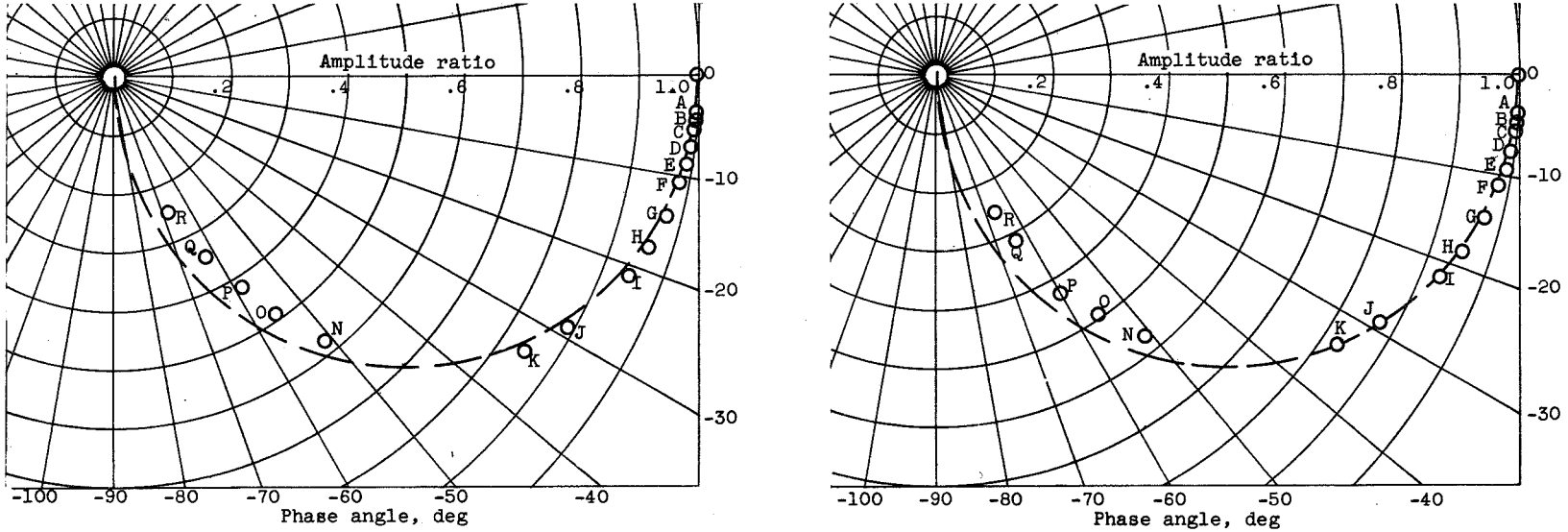

(a) Outer-spool speed.

(b) Inner-spool speed.

Figure 11. - Frequency-response curves for engine of different manufacturer.

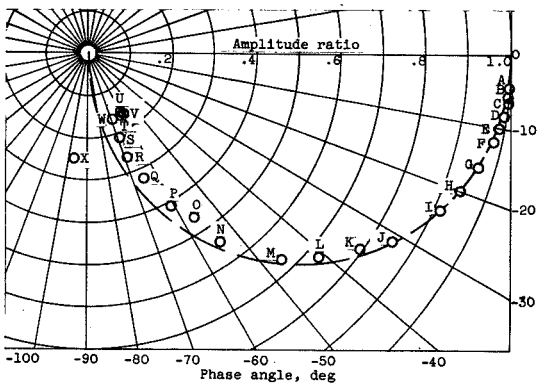

(a) Outer-spool speed.

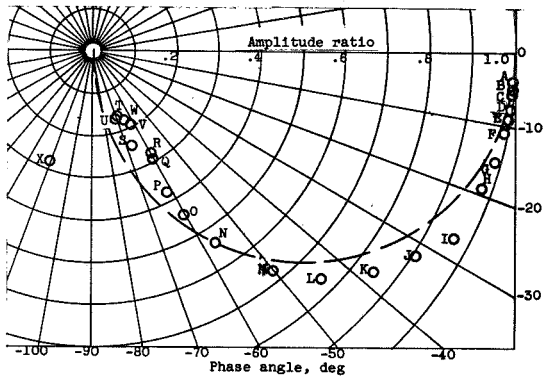

(b) Inner-spool speed.

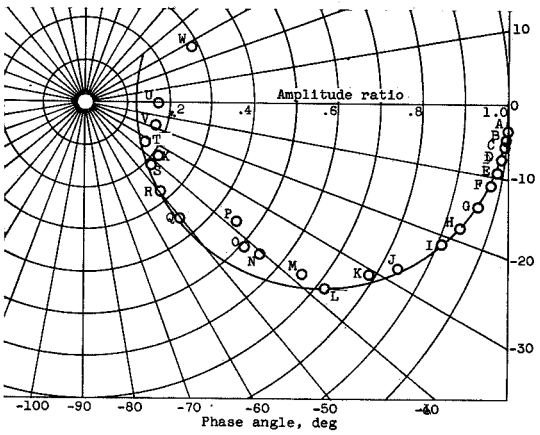

(c) Outer-compressor-discharge pressure.

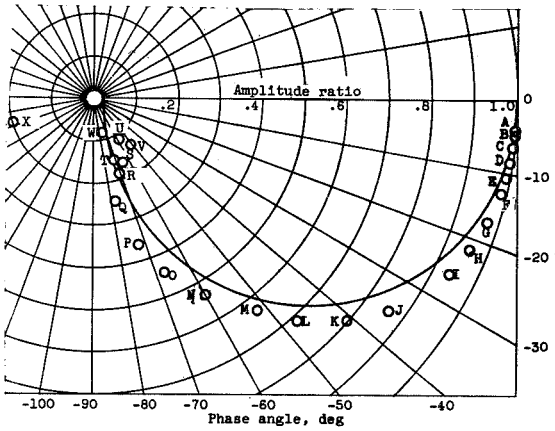

(d) Outer-compressor-discharge temperature.

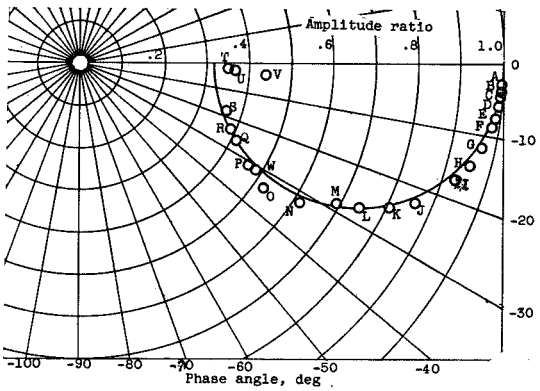

(e) Inner-compressor-discharge pressure.

Figure 12. - Frequency response of engine variables to change in turbine-inlet temperature for increase in corrected outer-spool speed from 87.5 to 92.9 percent rated and increase in corrected inner-spool speed from 93.5 to 96.1 percent rated. Bleed valves closed.

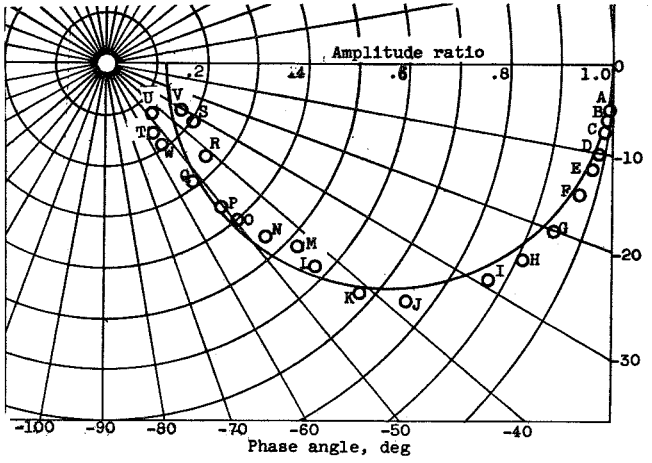

(f) Inner-compressor-discharge temperature.

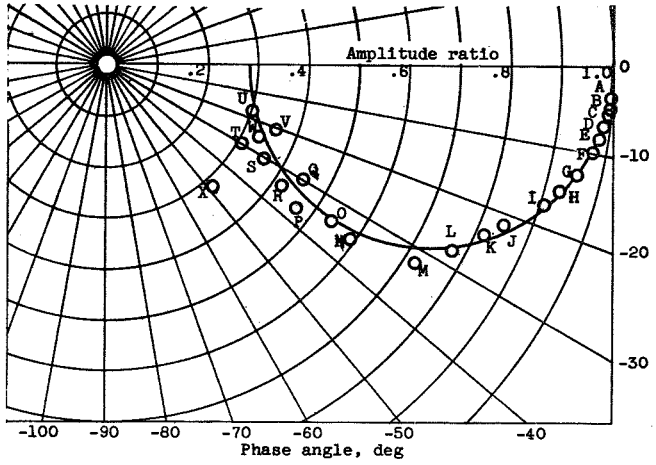

(g) Tail-pipe pressure.

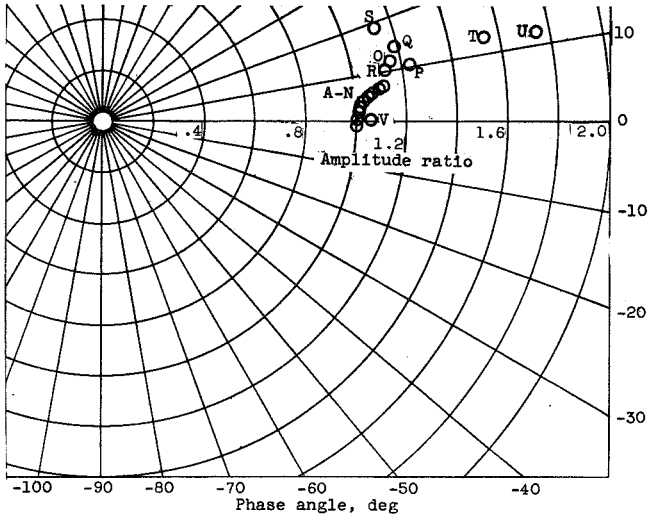

(h) Tail-pipe temperature.

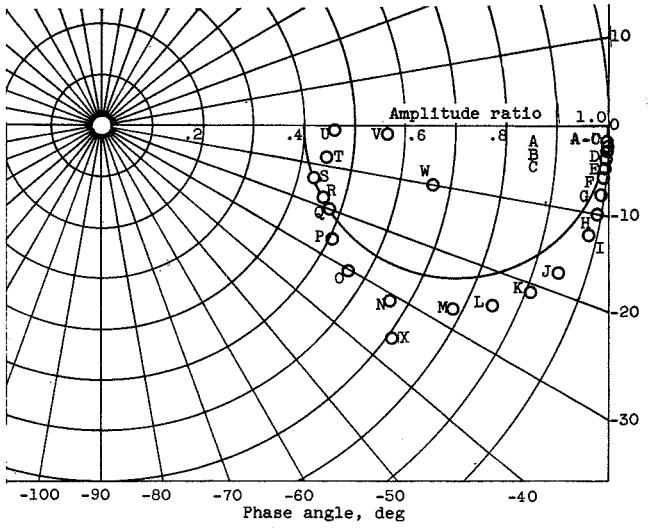

(i) Thrust.

Figure 12. - Concluded. Frequency response of engine variables to change in turbine-inlet temperature for increase in corrected outer-spool speed from 87.5 to 92.9 percent rated and increase in corrected inner-spool speed from 93.5 to 96.1 percent rated. Bleed valves closed.

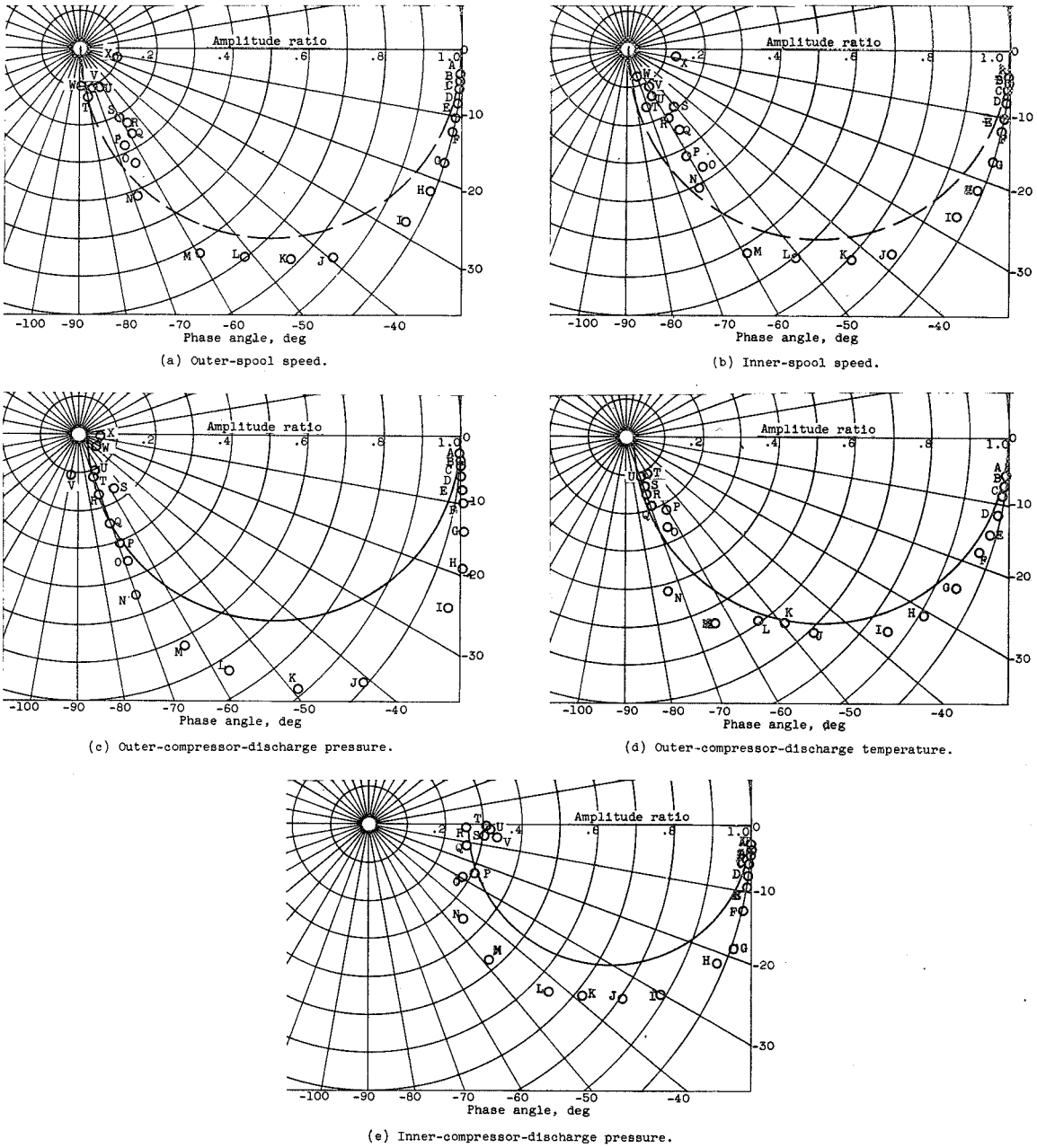

(a) Outer-spool speed.

(b) Inner-spool speed.

(c) Outer-compressor-discharge pressure.

(d) Outer-compressor-discharge temperature.

(e) Inner-compressor-discharge pressure.

Figure 13. - Frequency response of engine variables to change in turbine-inlet temperature for increase in corrected outer-spool speed from 57.6 to 62.9 percent rated and increase in corrected inner-spool speed from 79.6 to 82.5 percent rated. Bleed valves open.

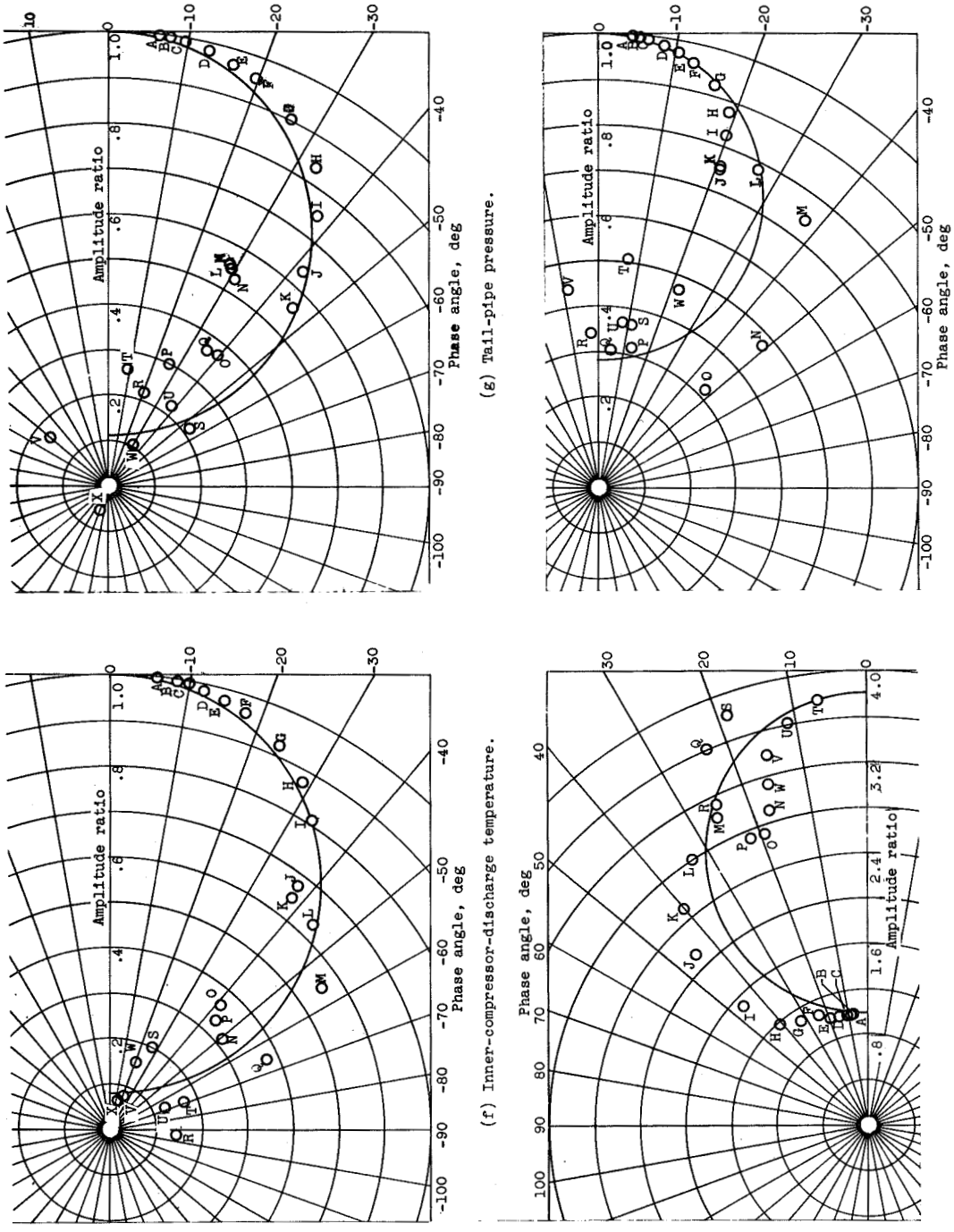

Figure 13. - Concluded. Frequency response of engine variables to change in turbine-inlet temperature for increase in corrected outer-spool speed from 57.6 to 62.9 percent rated and increase in corrected inner-spool speed from 79.6 to 82.5 percent rated. Bleed valves open.

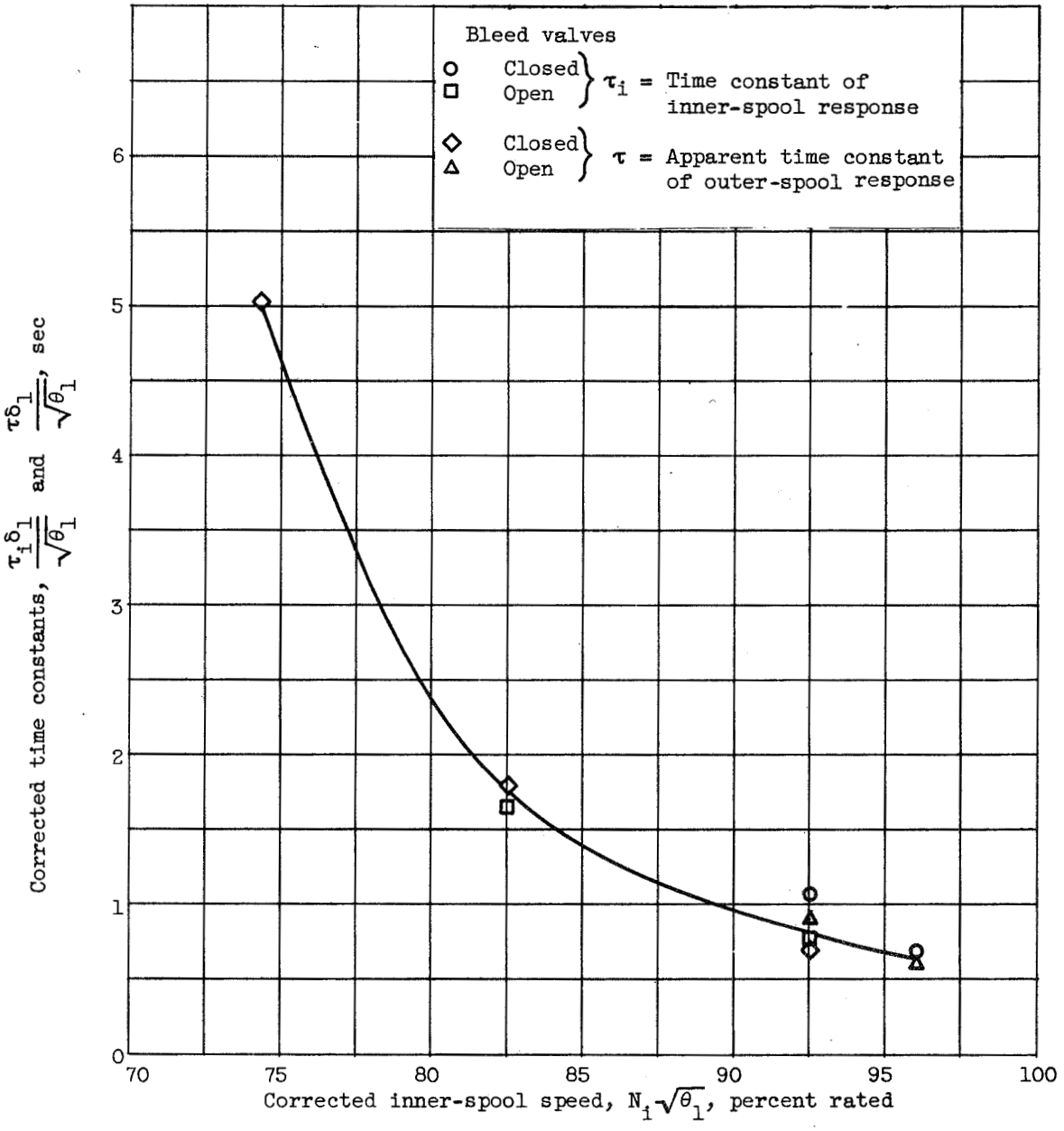

Figure 14. - Variation of spool time constants with engine speed for change in turbine-inlet temperature.

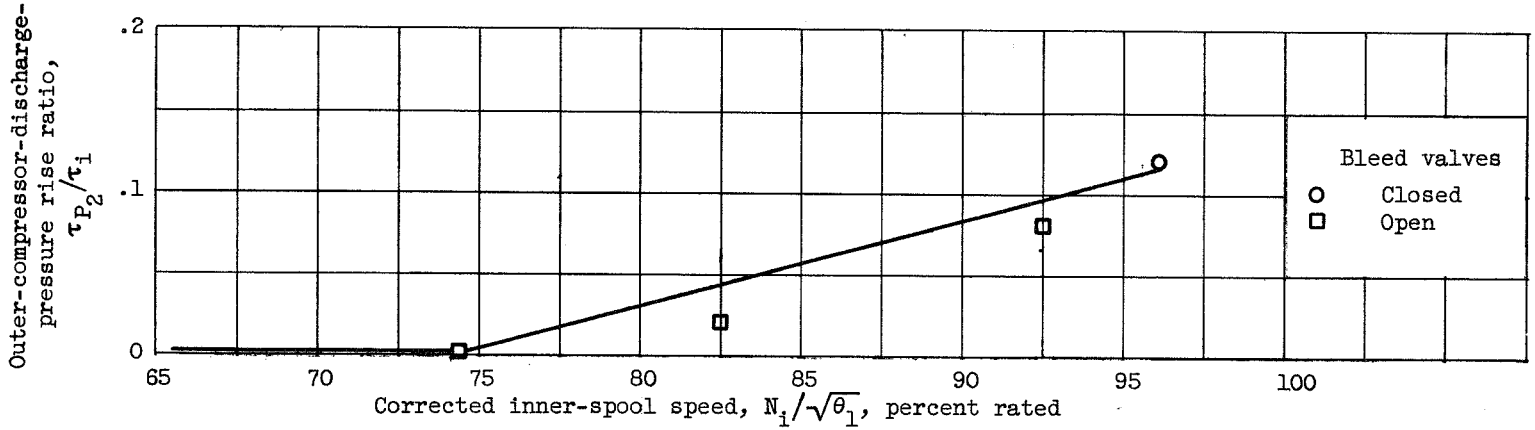

Figure 15. - Variation of outer-compressor-discharge-pressure rise ratio with engine speed for change in turbine-inlet temperature.

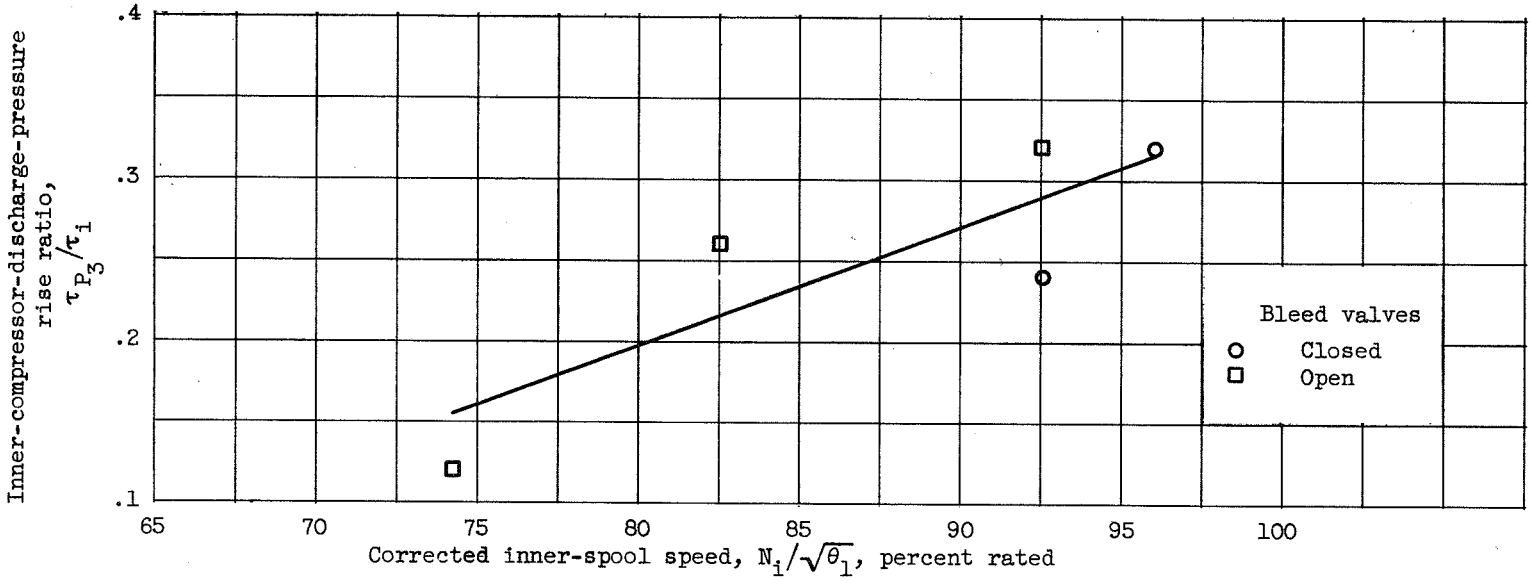

Figure 16. - Variation of inner-compressor-discharge-pressure rise ratio with engine speed for change in turbine-inlet temperature.

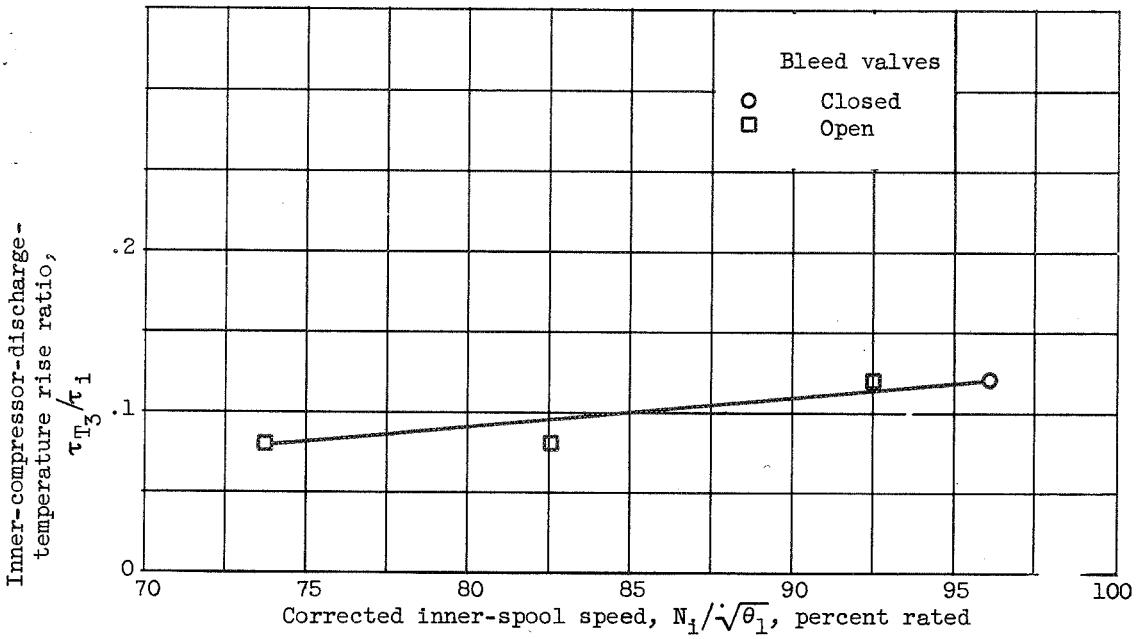

Figure 17. - Variation of inner-compressor-discharge-temperature rise ratio with engine speed for change in turbine-inlet temperature.

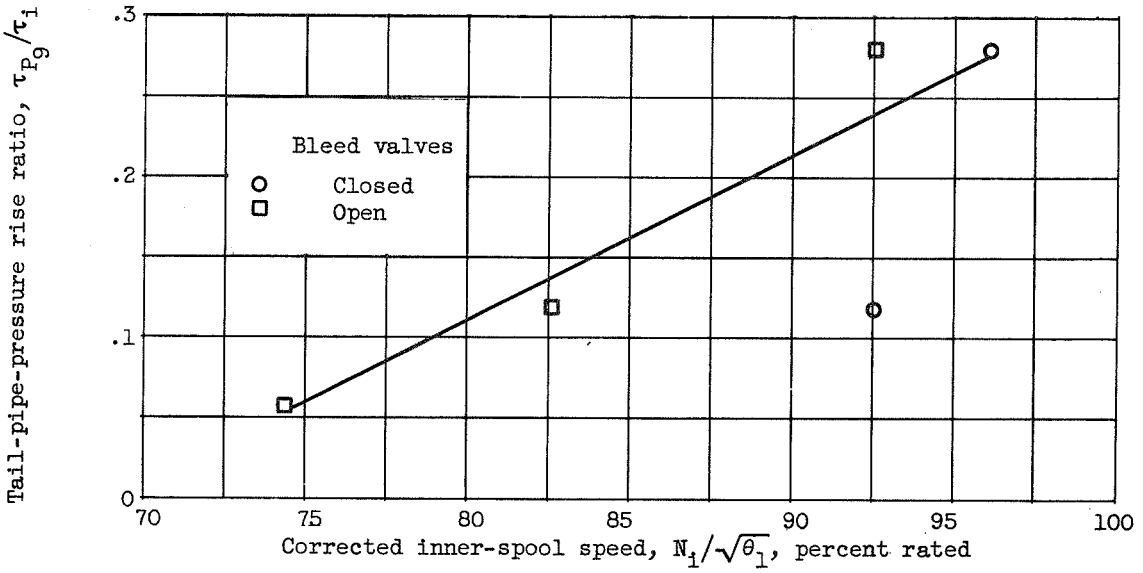

Figure 18. - Variation of tail-pipe-pressure rise ratio with engine speed for change in turbine-inlet temperature.

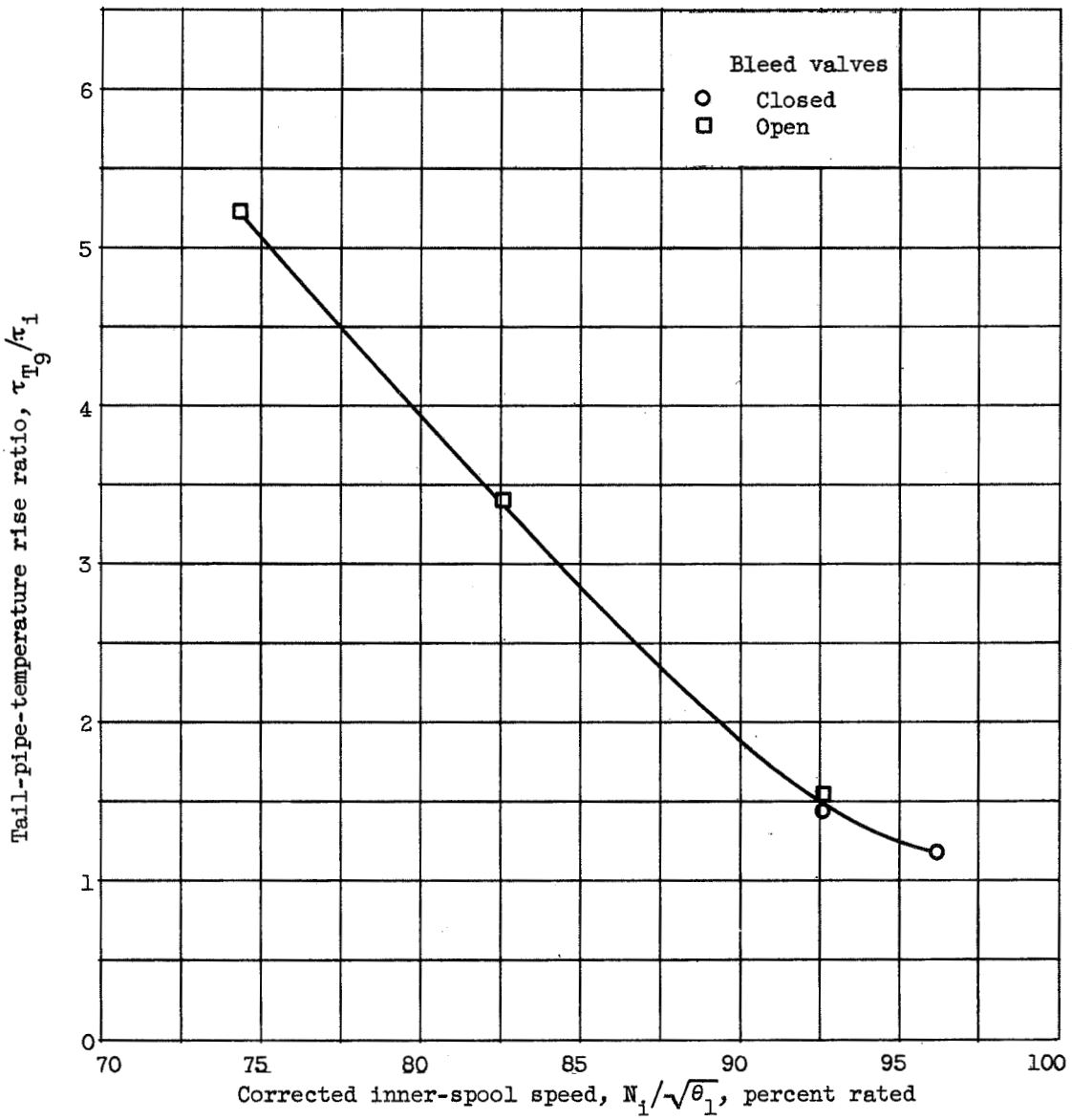

Figure 19. - Variation of tail-pipe-temperature rise ratio with engine speed for change in turbine-inlet temperature.

3485

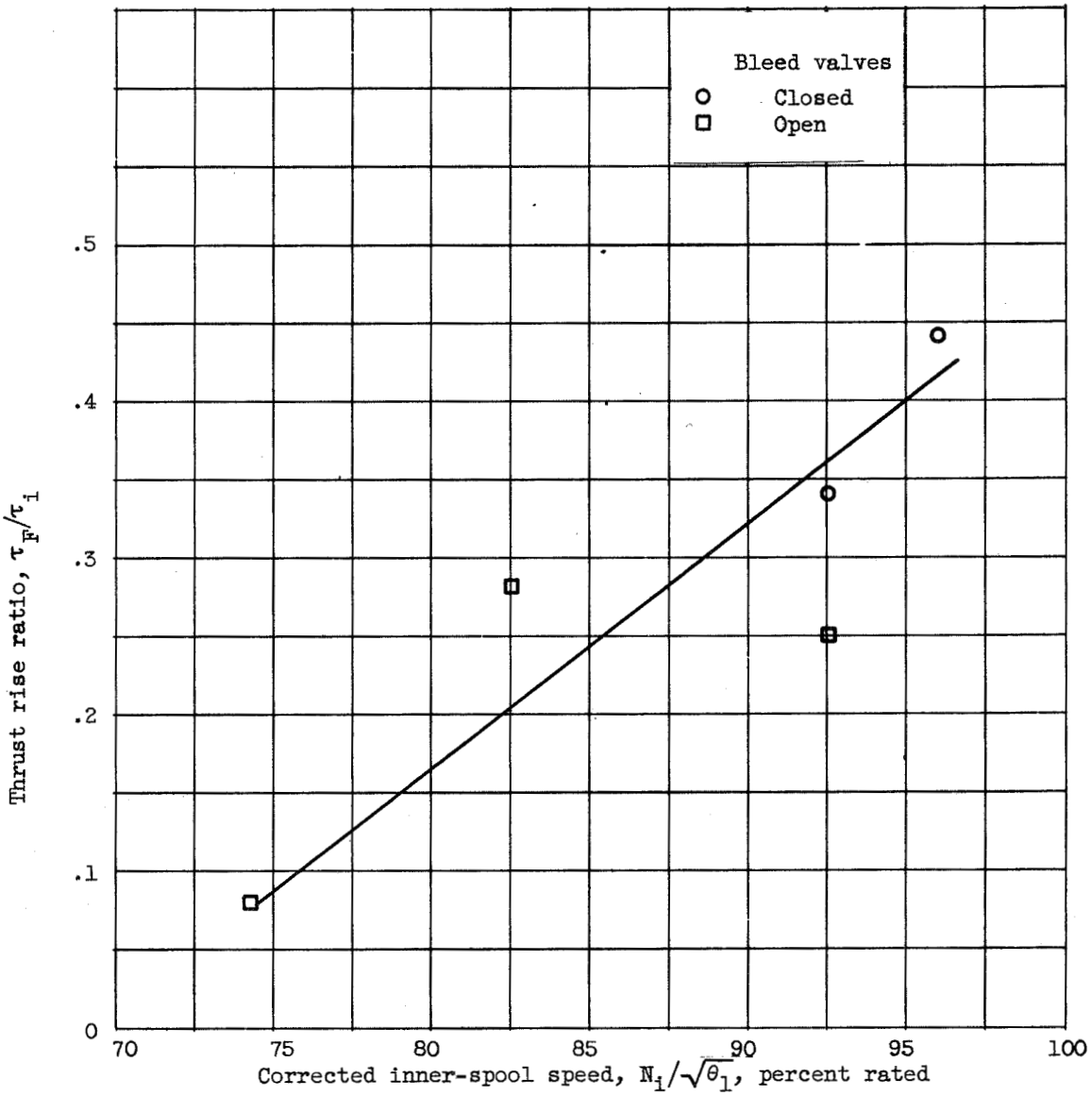

Figure 20. - Variation of thrust rise ratio with engine speed for change in turbine-inlet temperature.

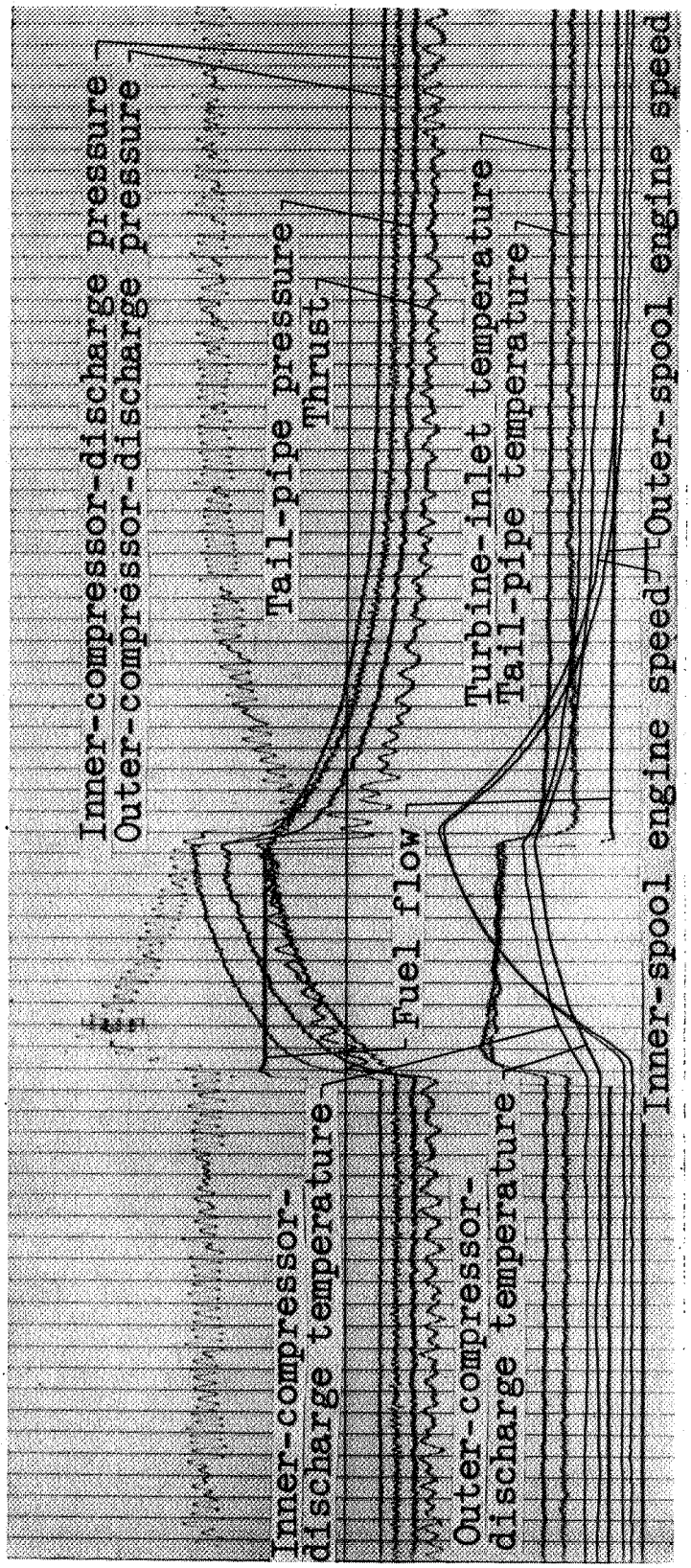

Figure 21. - Response of engine variables to large fuel step.

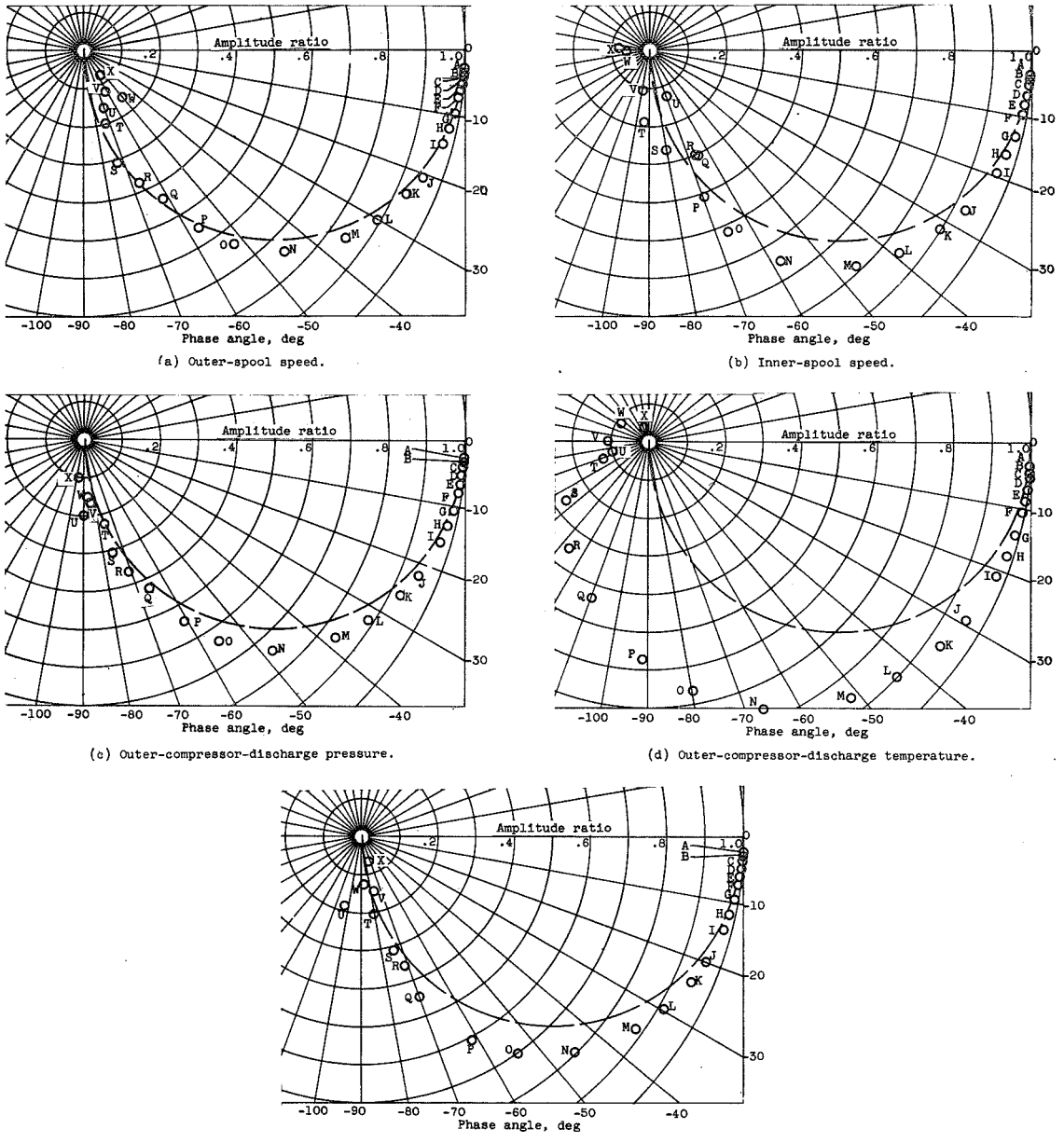

(a) Outer-spool speed.

(b) Inner-spool speed.

(c) Outer-compressor-discharge pressure.

(d) Outer-compressor-discharge temperature.

(e) Inner-compressor-discharge pressure.

Figure 22. - Frequency response of engine variables to change in exhaust-nozzle area for decrease in corrected outer-spool speed from 96.9 to 92.9 percent rated and increase in corrected inner-spool speed from 96.6 to 96.7 percent rated. Bleed valves closed.

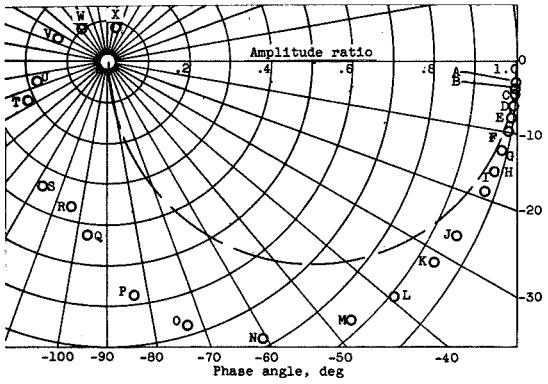

(f) Inner-compressor-discharge temperature.

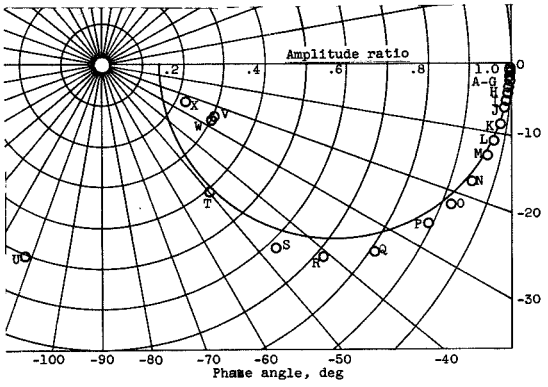

(g) Turbine-inlet temperature.

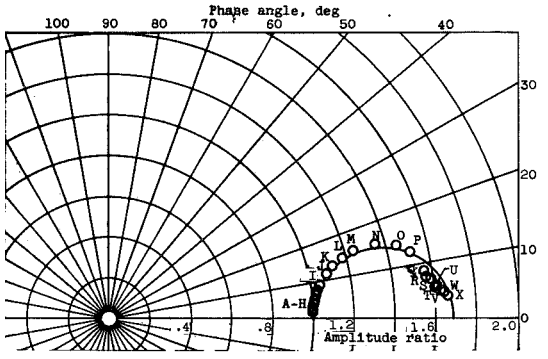

(h) Tail-pipe pressure.

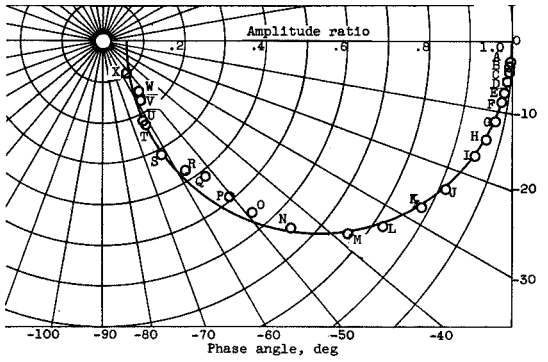

(i) Tail-pipe temperature.

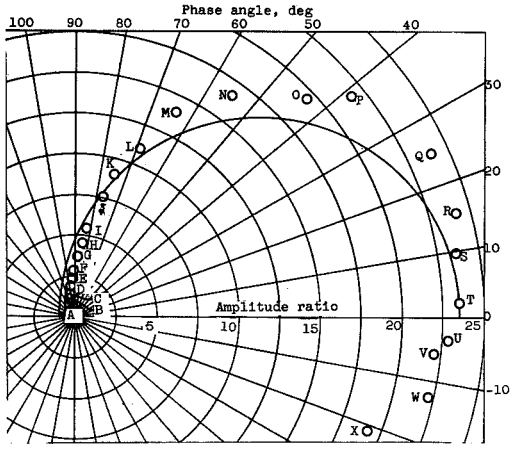

(j) Thrust.

Figure 22. - Concluded. Frequency response of engine variables to change in exhaust-nozzle area for decrease in corrected outer-spool speed from 96.9 to 92.9 percent rated and increase in corrected inner-spool speed from 96.6 to 96.7 percent rated. Bleed valves closed.

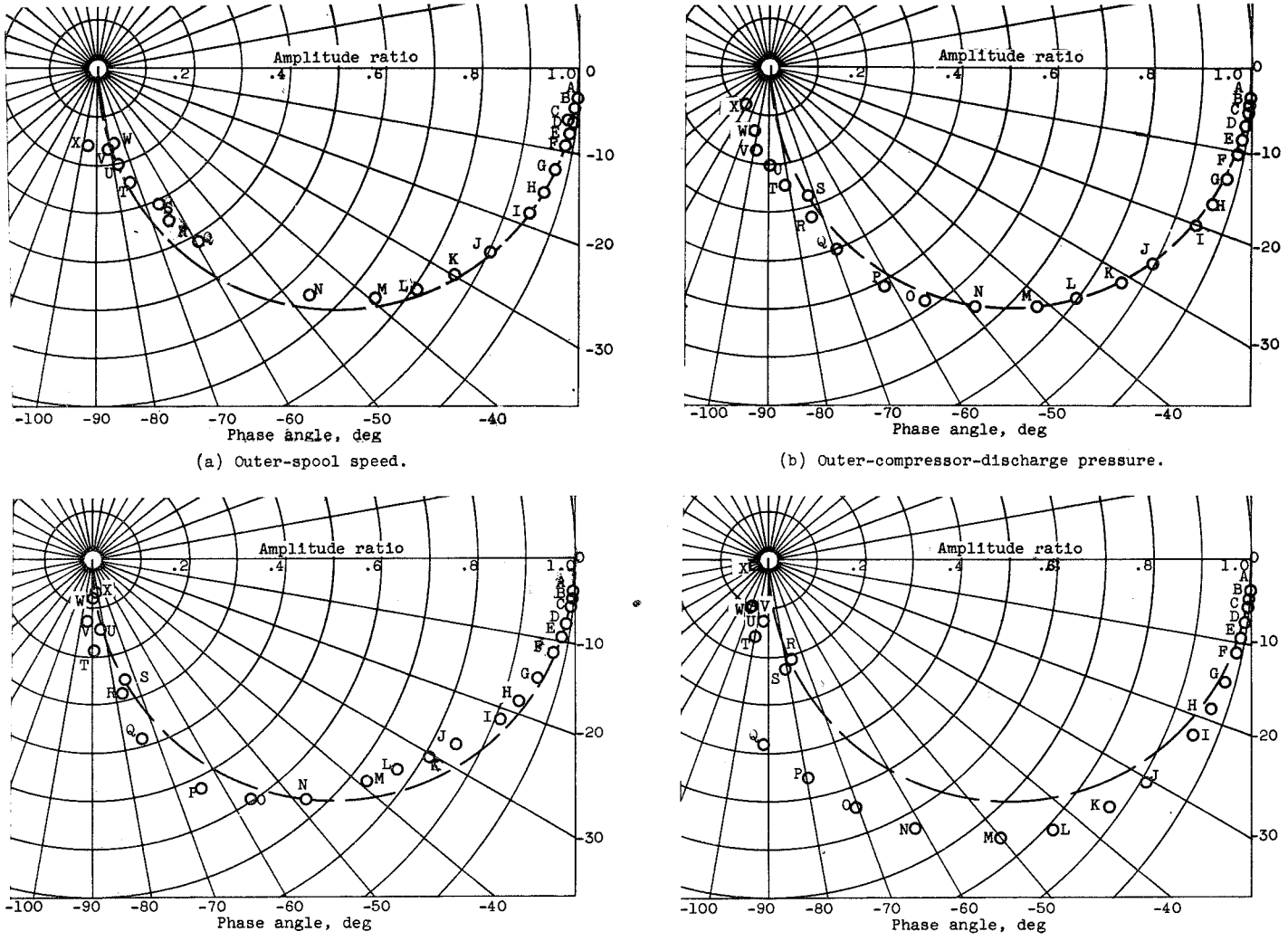

(a) Outer-spool speed.

(b) Outer-compressor-discharge pressure.

(c) Outer-compressor-discharge temperature.

(d) Inner-compressor-discharge pressure.

Figure 23. - Frequency response of engine variables to change in exhaust-nozzle area for decrease in corrected outer-spool speed from 88.0 to 85.1 percent rated and increase in corrected inner-spool speed from 92.9 to 93.0 percent rated. Bleed valves closed.

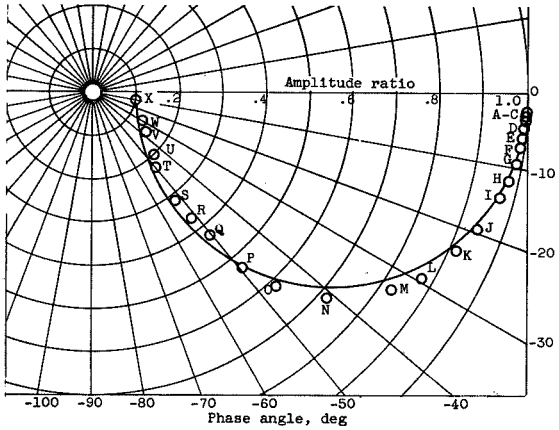

(e) Turbine-inlet temperature.

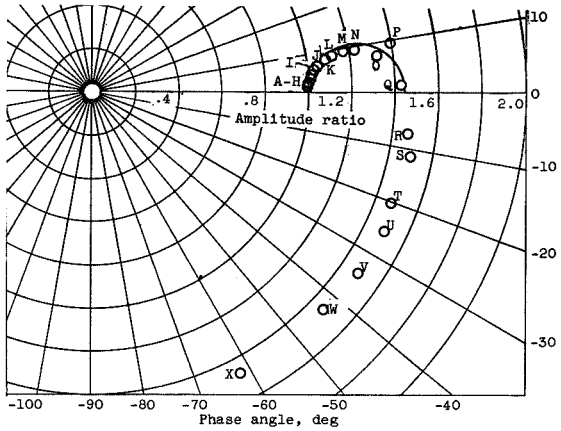

(f) Tail-pipe pressure.

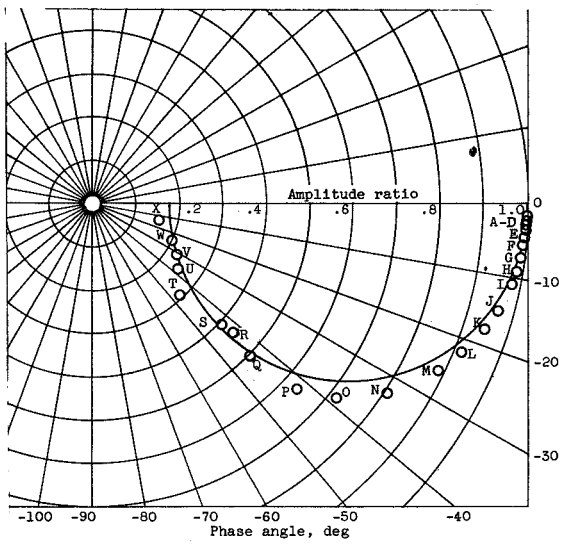

(g) Tail-pipe temperature.

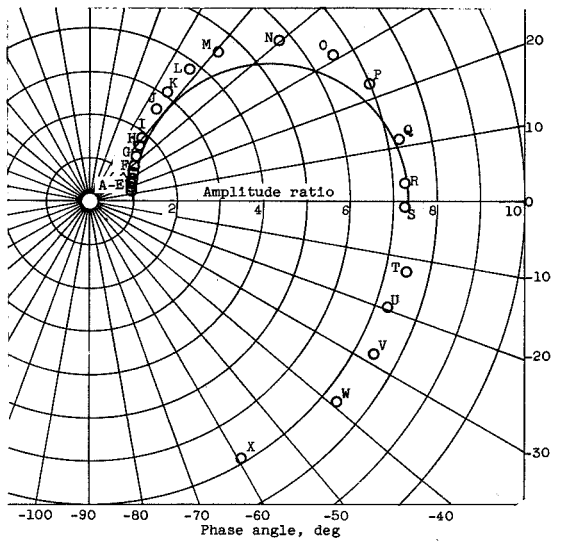

(h) Thrust.

Figure 23. - Concluded. Frequency response of engine variables to change in exhaust-nozzle area for decrease in corrected outer-spool speed from 88.0 to 85.1 percent rated and increase in corrected inner-spool speed from 92.9 to 93.0 percent rated. Bleed valves closed.

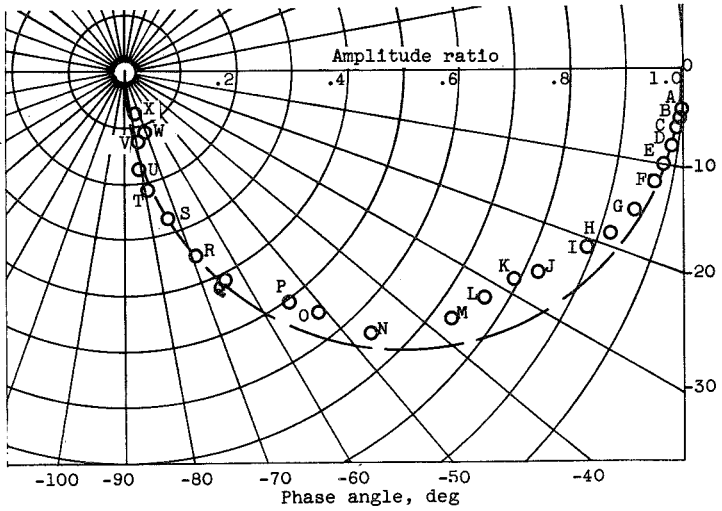

(a) Outer-spool speed.

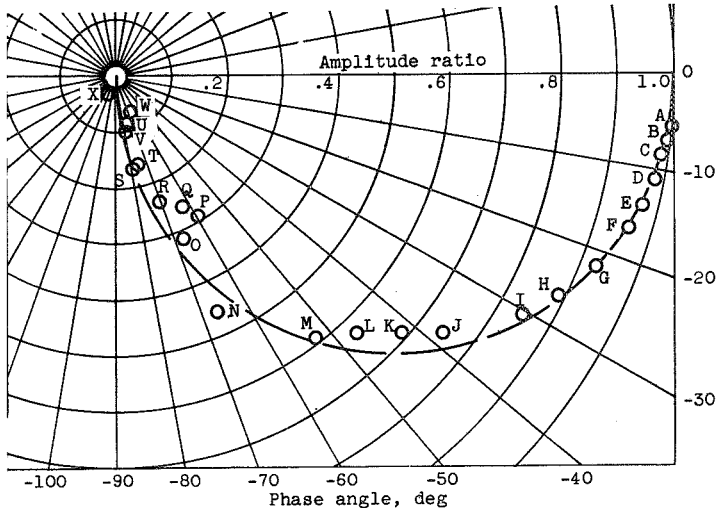

(b) Inner-spool speed.

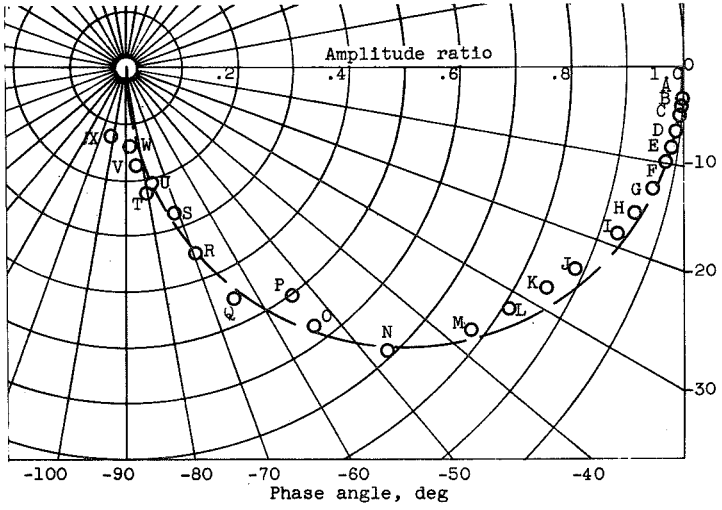

(c) Outer-compressor-discharge pressure.

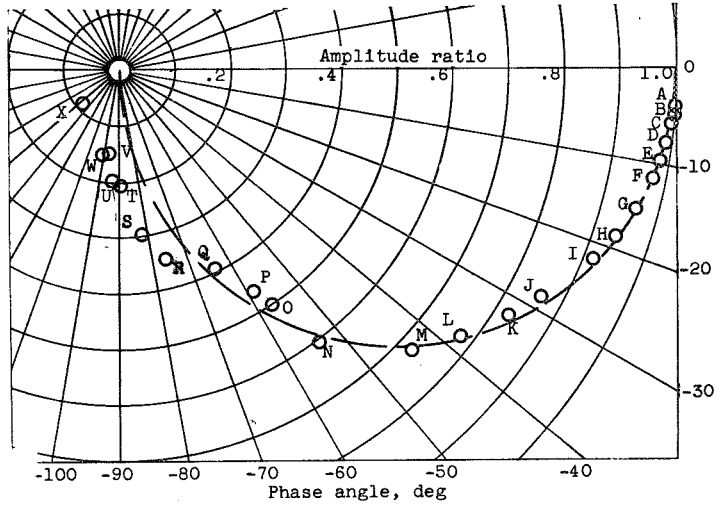

(d) Inner-compressor-discharge pressure.

Figure 24. - Frequency response of engine variables to change in exhaust-nozzle area for decrease in corrected outer-spool speed from 65.9 to 63.1 percent rated and decrease in corrected inner-spool speed from 83.8 to 83.1 percent rated. Bleed valves open.

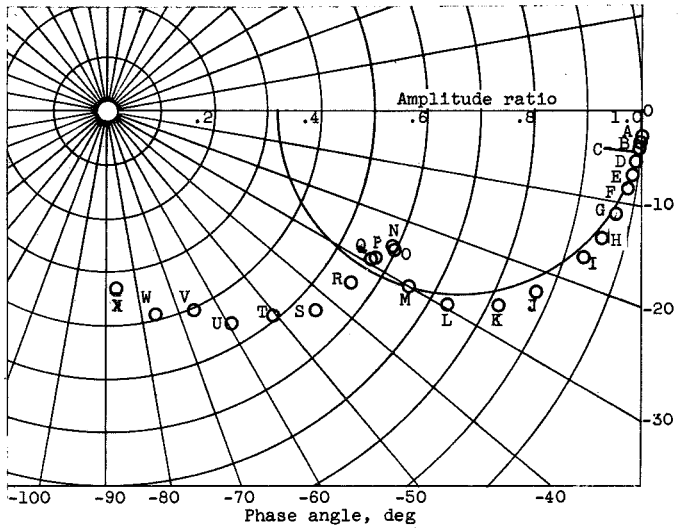

(e) Turbine-inlet temperature.

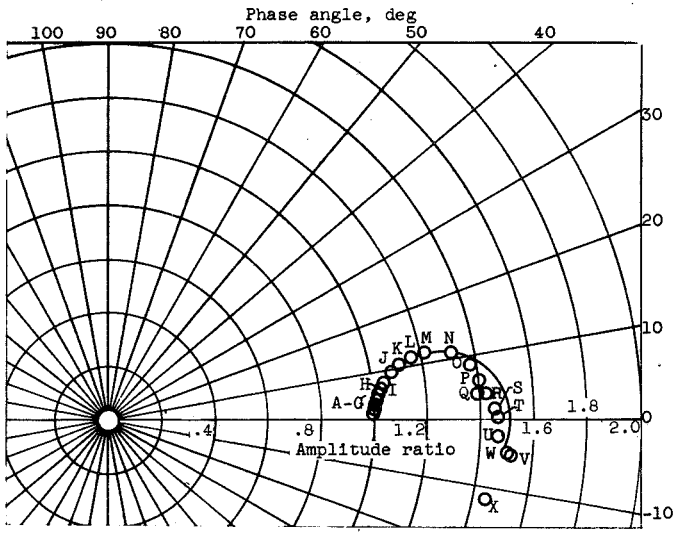

(f) Tail-pipe pressure.

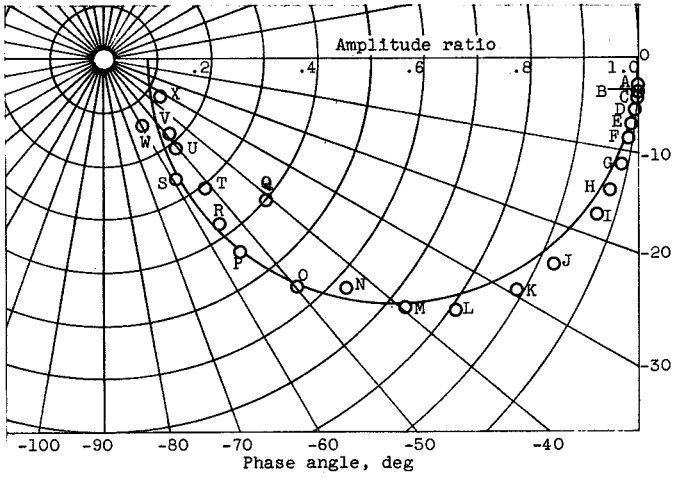

(g) Tail-pipe temperature.

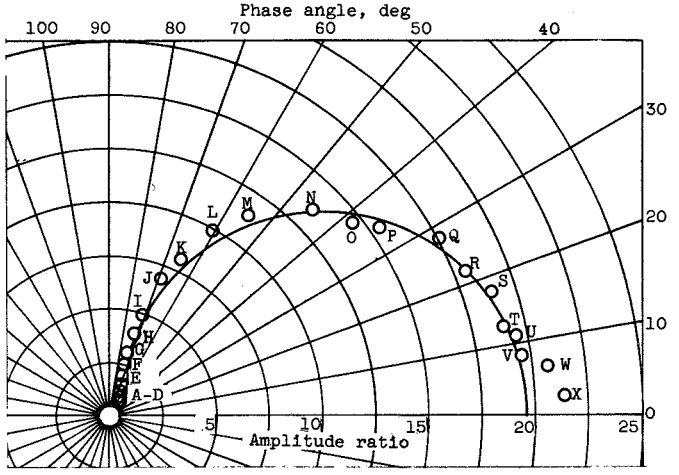

(h) Thrust.

Figure 24. - Concluded. Frequency response of engine variables to change in exhaust-nozzle area for decrease in corrected outer-spool speed from 65.9 to 63.1 percent rated and decrease in corrected inner-spool speed from 83.8 to 83.1 percent rated. Bleed valves open.

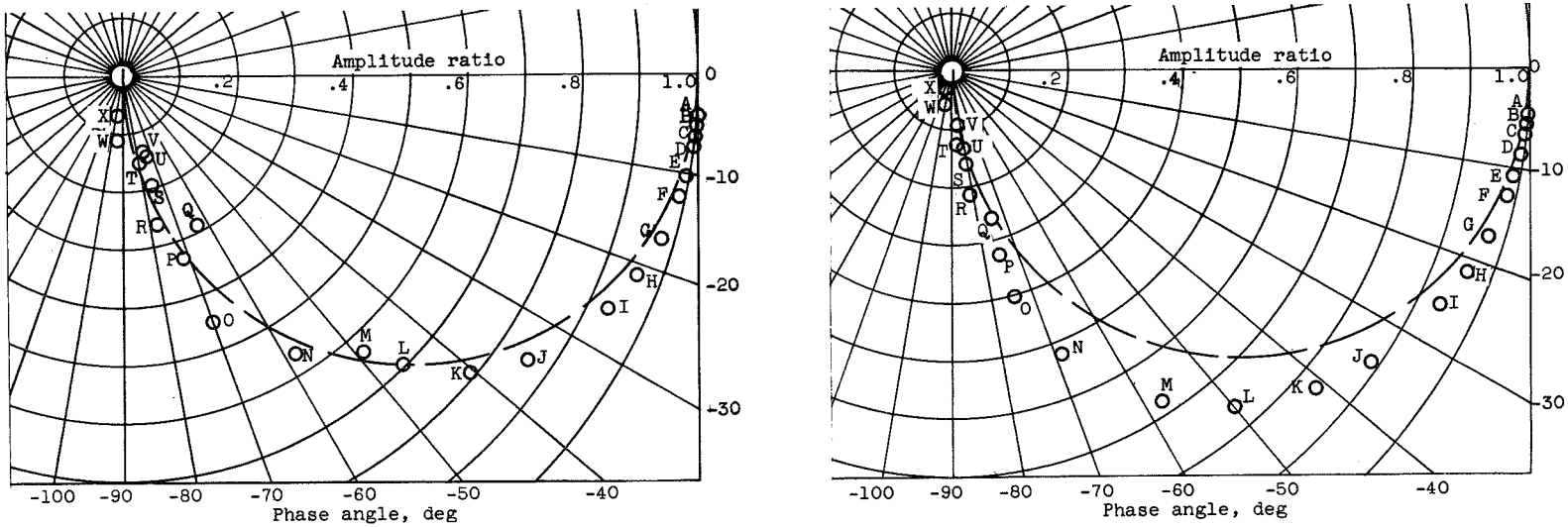

(a) Outer-spool speed.

(b) Inner-spool speed.

Figure 25. - Frequency response of engine variables to change in exhaust-nozzle area for decrease in corrected outer-spool speed from 46.4 to 44.7 percent rated and decrease in corrected inner-spool speed from 71.5 to 70.0 percent rated. Bleed valves open.

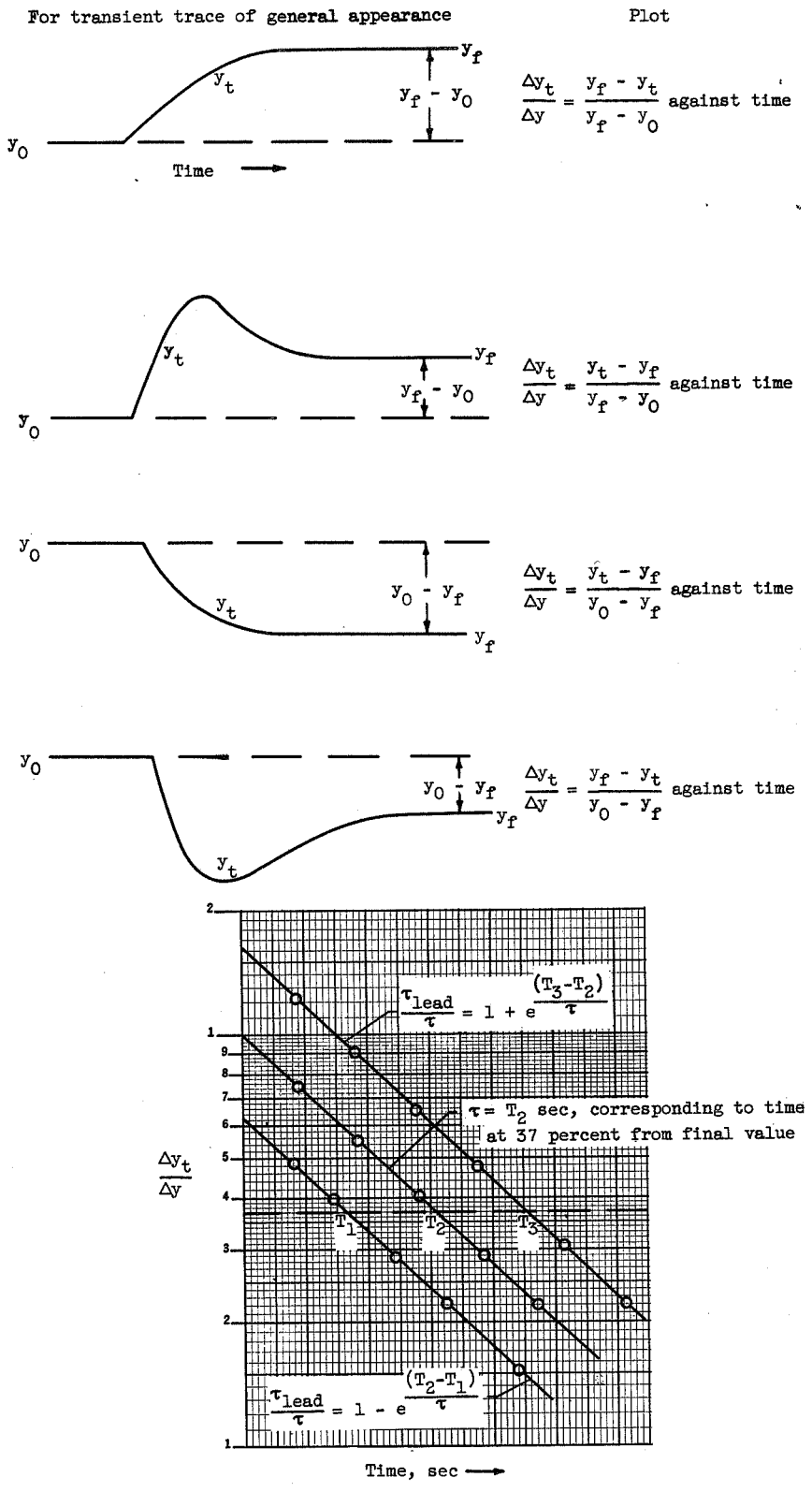

Figure 26. - Normalization of transient data for semilog plots (figs. 27 to 30).

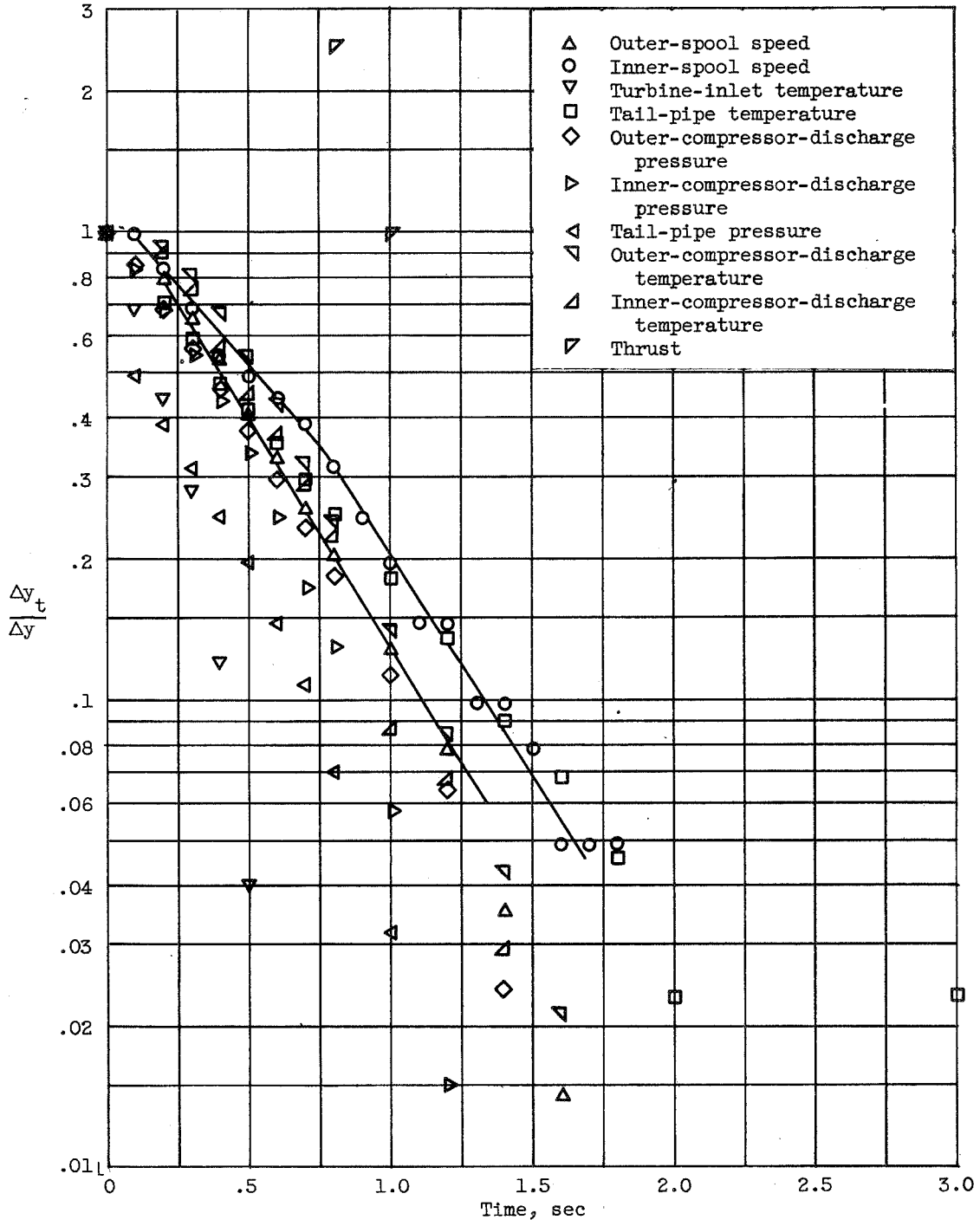

Figure 27. - Semilog plot of response of engine variables to change in exhaust-nozzle area for decrease in corrected outer-spool speed from 95.9 to 92.9 percent rated and increase in corrected inner-spool speed from 96.6 to 96.7 percent rated. Bleed valves closed.

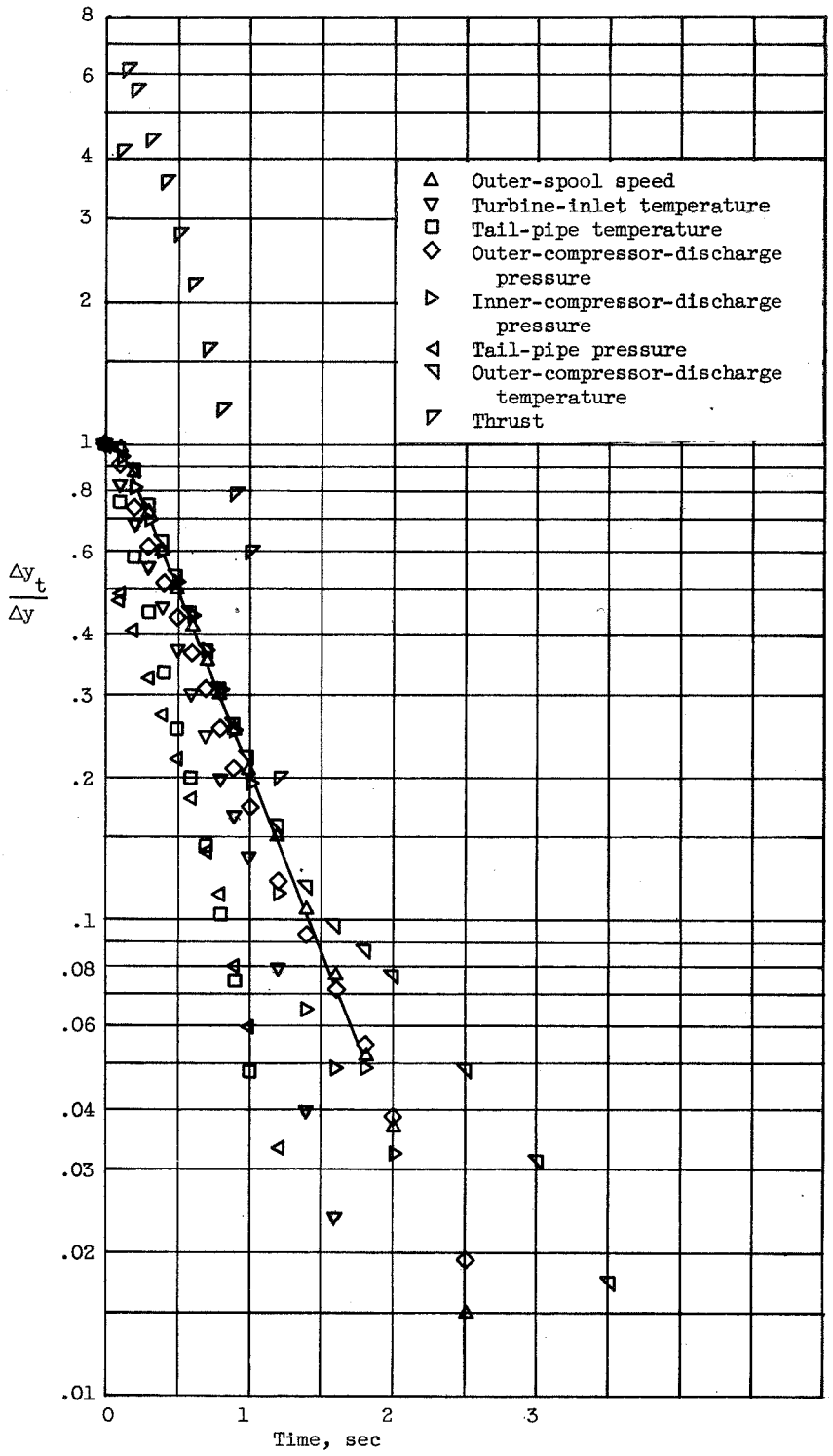

Figure 28. - Semilog plot of response of engine variables to change in exhaust-nozzle area for decrease in corrected outer-spool speed from 88.0 to 85.1 percent rated and increase in corrected inner-spool speed from 92.9 to 93.0 percent rated. Bleed valves closed.

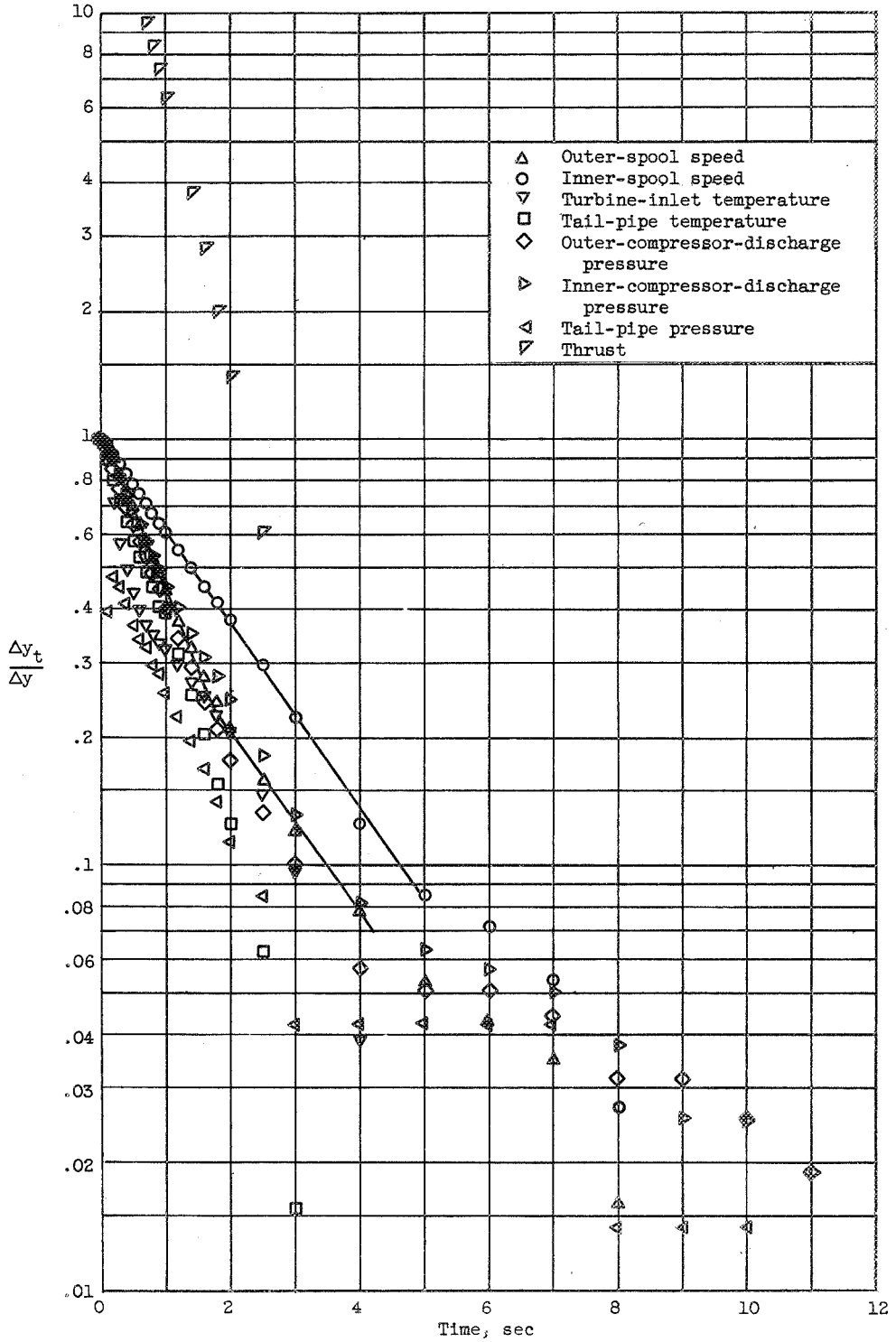

Figure 29. - Semilog plot of response of engine variables to change in exhaust-nozzle area for decrease in corrected outer-spool speed from 65.9 to 63.1 percent rated and decrease in corrected inner-spool speed from 83.8 to 83.1 percent rated. Bleed valves open.

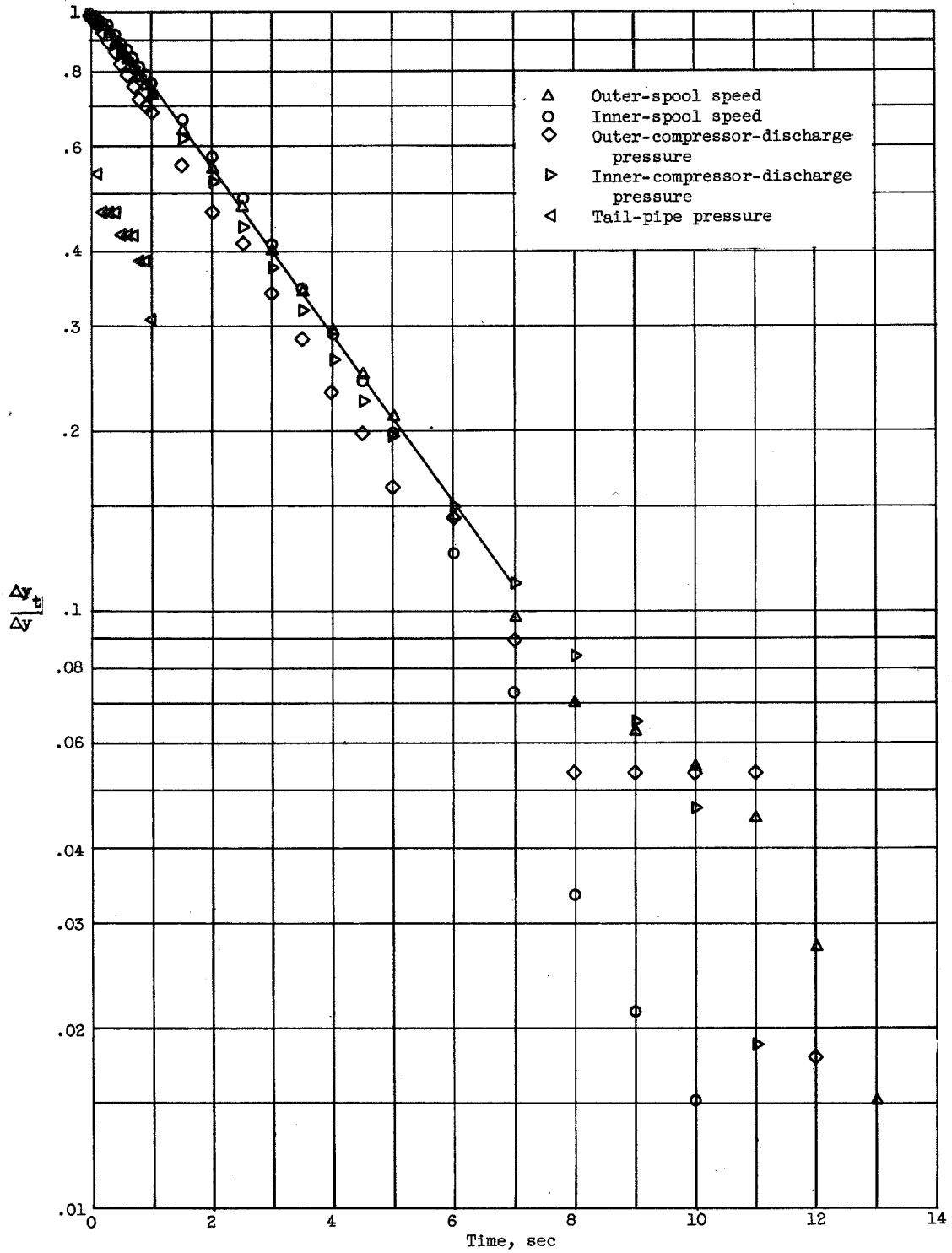

Figure 30. - Semilog plot of response of engine variables to change in exhaust-nozzle area for decrease in corrected outer-spool speed from 46.4 to 44.7 percent rated and decrease in corrected inner-spool speed from 71.5 to 70.0 percent rated. Bleed valves open.

3485

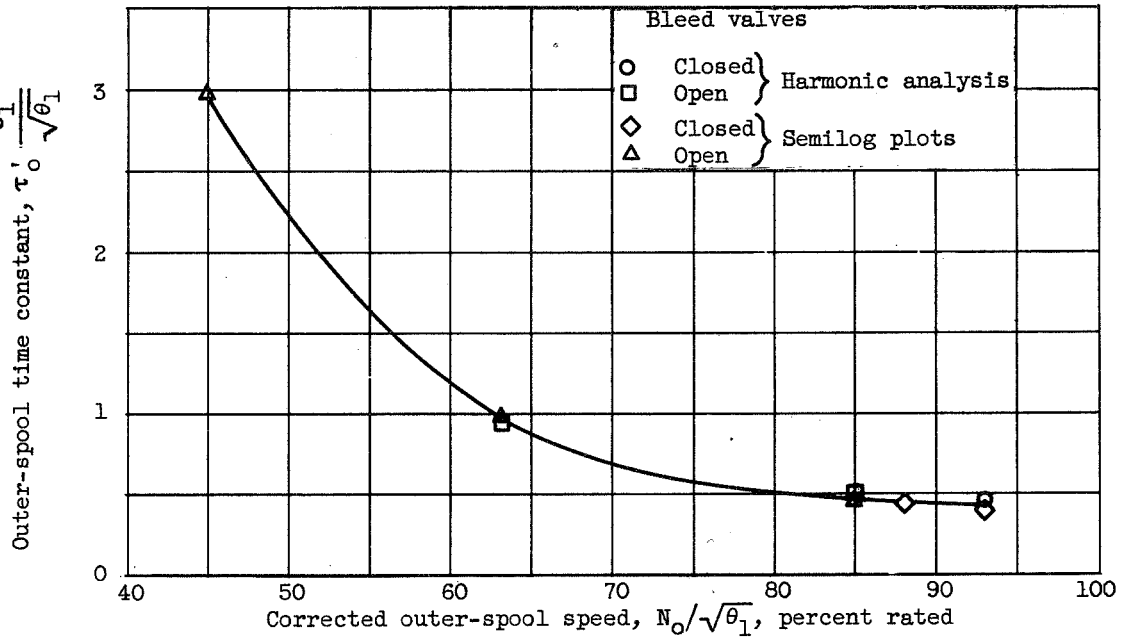

Figure 31. - Variation of outer-spool time constant with engine speed for change in exhaust-nozzle area.

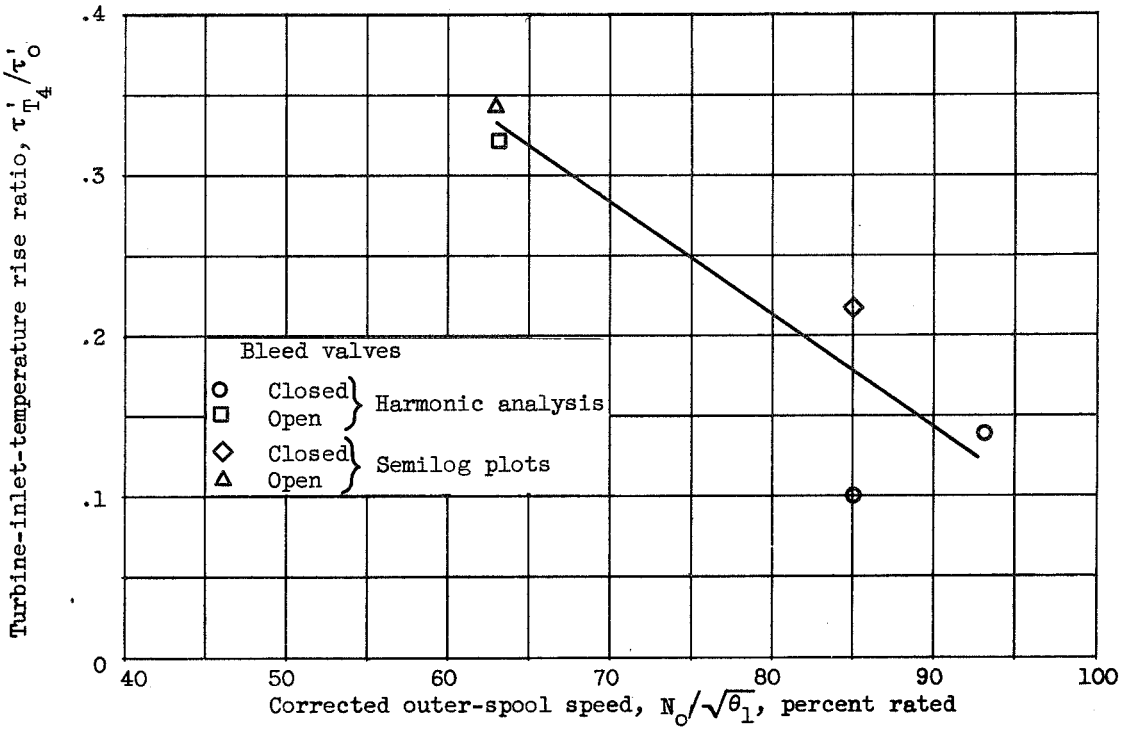

Figure 32. - Variation of turbine-inlet-temperature rise ratio with engine speed for change in exhaust-nozzle area.

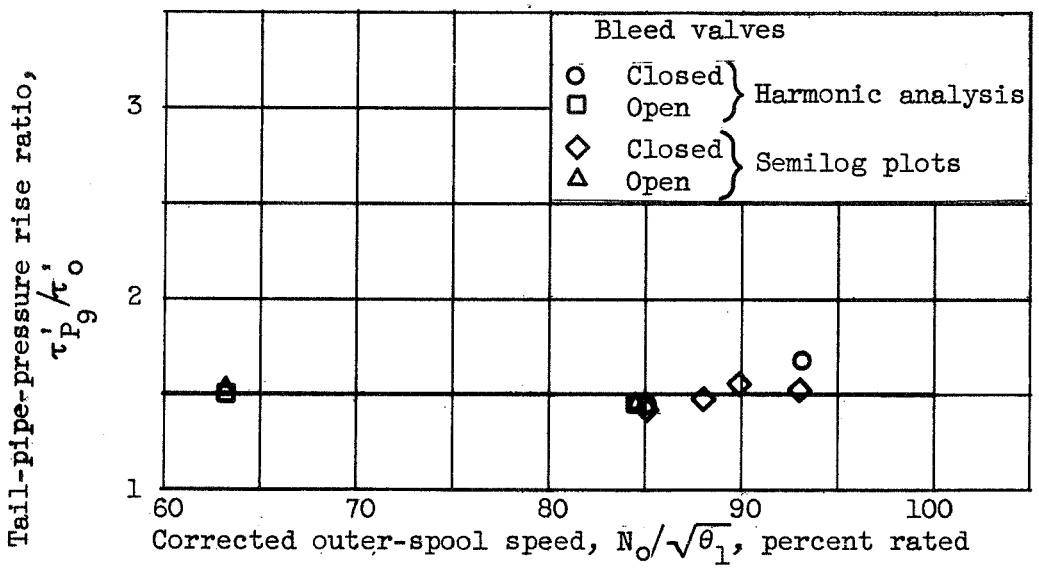

Figure 33. - Variation of tail-pipe-pressure rise ratio with engine speed for change in exhaust-nozzle area.

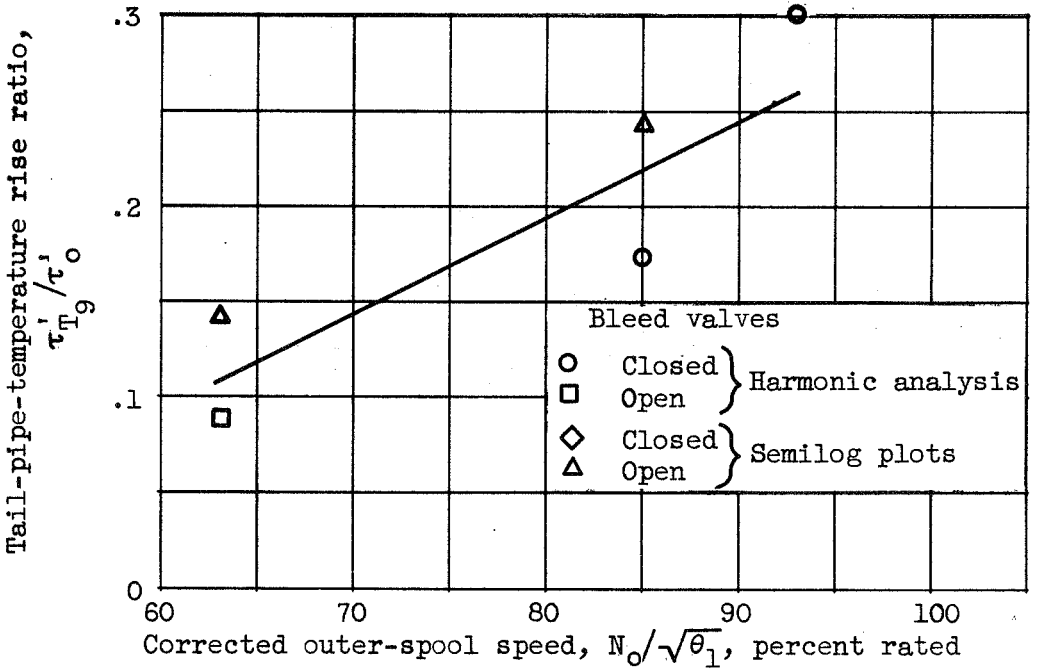

Figure 34. - Variation of tail-pipe-temperature rise ratio with engine speed for change in exhaust-nozzle area.

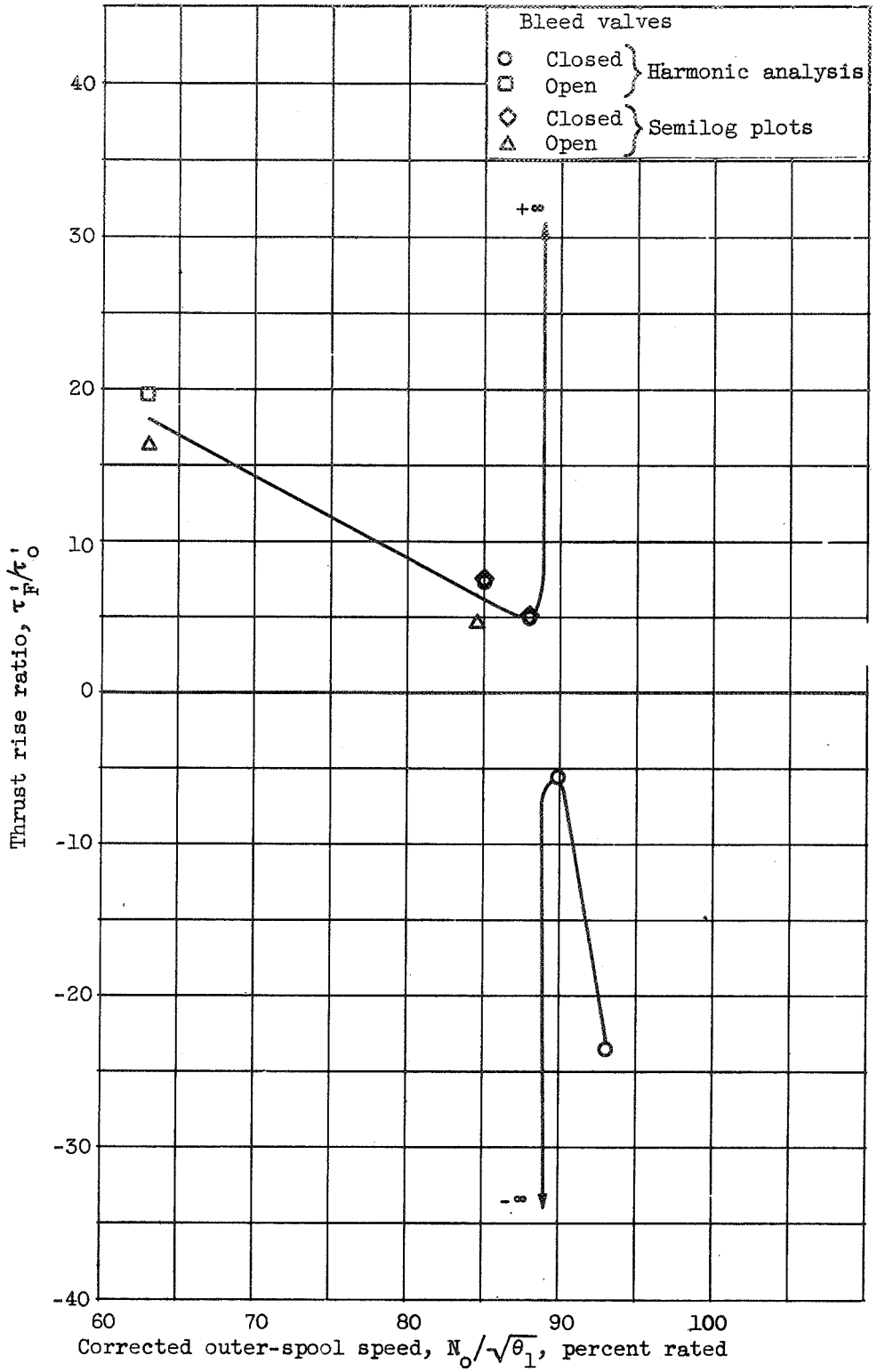

Figure 35. - Variation of thrust rise ratio with engine speed for change in exhaust-nozzle area.

EXPERIMENTAL DETERMINATION OF LINEAR DYNAMICS OF TWO-SPOOL TURBOJET ENGINES

David Novik
Aeronautical Research Scientist
Propulsion Systems

Herbert Heppler
Aeronautical Research Scientist
Propulsion Systems

Approved:

John C. Sanders
Aeronautical Research Scientist
Propulsion Systems

Bruce T. Lundin
Chief
Engine Research Division

amk - 10/19/54

Engines, Turbojet 3.1.3

Engines, Control - Turbojet 3.2.2

Novik, David, and Heppler, Herbert

EXPERIMENTAL DETERMINATION OF LINEAR DYNAMICS OF TWO-SPOOL TURBOJET ENGINES

Abstract

Transfer functions descriptive of the response of most engine variables were determined from transient data that were obtained from approximate step inputs in fuel flow and in exhaust-nozzle area. The speed responses of both spools to fuel flow and to turbine-inlet temperature appeared as identical first-order lags. Response to exhaust-nozzle area was characterized by a first-order lag response of the outer-spool speed, accompanied by virtually no change in inner-spool speed.